# COMPARISON OF LINEAR AND CFD MODELS WITH ON-SITE WIND MEASUREMENT DATA FOR WIND RESOURCE ASSESSMENT

**A Thesis Submitted to**
**the Graduate School of Engineering and Sciences of**
**İzmir Institute of Technology**
**in Partial Fulfillment of the Requirements for the Degree of**

**MASTER OF SCIENCE**

**in Mechanical Engineering**

**by**
**Aytek AY**

**January 2014**
**İZMİR**

We approve the thesis of **Aytek AY**

**Examining Committee Members:**

**Prof. Dr. M. Barış ÖZERDEM**
Department of Energy Systems Engineering, Bahçeşehir University

**Assoc. Prof. Dr. Moghtada MOBEDI**
Department of Mechanical Engineering, Izmir Institute of Technology

**Prof. Dr. Aydoğan ÖZDAMAR**
Department of Mechanical Engineering, Ege University

**10 January 2014**

**Prof. Dr. M. Barış ÖZERDEM**
Supervisor, Department of Energy Systems Engineering,
Bahçeşehir University

**Prof. Dr. Metin TANOĞLU**
Head of Department of Mechanical Engineering

**Prof. Dr. R. Tuğrul SENGER**
Dean of the Graduate School of Engineering and Science

# ACKNOWLEDGMENTS

I would like to express my deepest gratitude to my advisor Prof.Dr.Barış ÖZERDEM for his guidance, support and patience.

I would like to thank to Çağdaş ÜNVEREN, Şule ERKOÇ and Mahir TOSUN for sharing their visions, giving me the excitement of working in the wind business and for their valuable friendship.

I would like to thank to Mark Burgdorf HERSKIND and Georg BISCHOF for their continuous supports and guidance.

I would like to thank to Iñigo Maña ROBREDO, Melanie STOCK and Ingo HIRSCHHAUSEN for their former guidance about siting and friendship.

I would like to thank to Simla TANRIVERDİ for supporting and encouraging me by always being there.

And finally I would like to express my sincere gratitude to my family for their love and support which have always braced me up.

# ABSTRACT


## COMPARISON OF LINEAR AND CFD MODELS WITH ON-SITE WIND MEASUREMENT DATA FOR WIND RESOURCE ASSESSMENT

Wind resource assessment (WRA) estimates the strength of wind resources at a planned wind project site. The output of WRA is wind conditions and annual energy production at a wind project site. The aim of this study is to compare on-site measurements with a linear and non-linear flow model results by calculating the error values between and investigating the effects on the annual energy productions. Wind Atlas Analysis and Application Program (WAsP) is used for linear model approach, whilst software called WindSim is used for non-linear model approach based on computational fluid dynamics (CFD) concept. Relative and absolute wind speed errors which have been weighted with the frequency of the directions show that the CFD model gives better results. This non-linear model also leads in annual energy predictions with 1.8% relative error averaged over three met mast results which is 4.2% for linear model. Although non-linear results seem to be better in such a semi-complex site as a further study it is important to run several more test cases for sites with different complexity and stability conditions.

The results of non-linear model have been obtained with a new post-processing tool created by Siemens Wind Power. It is also necessary to run the same calculation procedure for several more complex sites before using as a standard tool as this is the first test case of this calculation method.

# ÖZET

## RÜZGAR KAYNAĞI BELİRLEMEDE SAHADA ÖLÇÜLEN RÜZGAR VERİLERİ İLE LİNEER VE CFD MODELLERİNİN KARŞILAŞTIRILMASI

Rüzgar santrallerinin kurulması düşünülen yerlerde proje öncesi rüzgar kaynağı değerlendirmesi yapılarak sahanın yıllık potensiyel enerji üretimleri elde edilebilmektedir. Bu çalışmada da lineer ve non-lineer akış modellerinin sonuçları için hata değerleri hesaplanmış ve yıllık enerji üretimi üzerindeki etkilerinin ne olduğunun araştırılması amaçlanmıştır. Lineer model hesaplamaları için Rüzgar Atlası Analiz ve Hesaplama Programı (WAsP) kulanılırken non-lineer model için Hesaplamalı Akışkanlar Dinamiği (HAD) çözümlemesi yapan WindSim yazılımı kullanılmıştır. Non-lineer model ile elde edilen rüzgar hızlarının ölçüme göre olan bağıl ve mutlak hata oranları lineer model sonuçlarına göre daha düşüktür. Üç ölçüm direği noktasındaki yıllık enerji üretimlerinin ortalaması kıyaslandığında da non-lineer model sonuçları gerçek ölçümle hesaplanan üretime göre %1.8 'lik bir sapmayla %4.2 olan lineer model sapmasından daha iyi sonuç vermektedir. Her ne kadar yarı-kompleks sayılabilecek olan mevcut sahadaki sonuçlar non-lineer model için gerçek değerlere daha yakın çıksa da farklı zorluklarda (komplekslikler) ve atmosferik stabilite durumlarındaki sahalarda da aynı yöntemin test edilmesi önem teşkil etmektedir.

Non-lineer model sonuçları, hesaplamaların yapılmasından sonra Siemens Wind Power tarafından geliştirilen bir art işlem (post-processing) yazılımı kullanılarak elde edilmiştir. Mevcut çalışma, bu yazılımın denendiği ilk uygulama olduğu için standart olarak kullanılmadan önce daha zorlu olan birkaç farklı sahada denenmesi ve sonuçlarının incelenmesi gerekmektedir.

# TABLE OF CONTENTS

# LIST OF FIGURES

**Figure**

**Page**

# LIST OF TABLES

**Figure**

**Page**

# LIST OF SYMBOLS

| | |
|---|---|
| A | Designated parameter for higher turbulence characteristic |
| B | Designated parameter for medium turbulence characteristic |
| C | Designated parameter for lower turbulence characteristic |
| e | Elongating deformation |
| $e_{abs}$ | Absolute error |
| $e_{rel}$ | Relative error (%) |
| f | Frequency (Hz) |
| $I_{ref}$ | Turbulence intensity at 15 m/s |
| L | Monin-Obukhov length (m) |
| P | Mean static pressure ($N/m^2$) |
| S | Reynold's stress tensor n (N/kg) |
| t | Time (s) |
| u' | Fluctuating velocity (m/s) |
| $u_*$ | Friction velocity (m/s) |
| U | Mean velocity (m/s) |
| $U^m$ | Measured mean wind speed (m/s) |
| $U^p$ | Predicted mean wind speed (m/s) |
| $V_{e50}$ | 3 sec. gust with a recurrence period of 50 years (m/s) |
| Vref | 10 min mean wind speed with a recurrence period of 50 years (m/s) |
| x | Position vector |
| z | height (m) |
| $z_0$ | Roughness length (m) |
| $z_{hub}$ | Hub height of the WTG type (m) |
| α | Wind shear exponent |
| ε | Turbulence dissipation rate ($m^2/s^3$) |
| η | Kolmogorov length scale (m) |
| κ | Von Karman constant |
| λ | Second viscosity (kg/s*m) |
| μ | First (dynamic) viscosity (kg/s*m) |

| | |
|---|---|
| $\rho$ | Density ($kg/m^3$) |
| $\tau$ | Viscous stress component (Pa) |
| $\Psi$ | Empirical function of the atmospheric stability condition |

# LIST OF ABBREVIATIONS

| | |
|---|---|
| ABL | Atmosheric Boundary Layer |
| AEP | Annual Energy Production |
| a.g.l. | Above Ground Level |
| CF | Coriolis Force |
| CFD | Computational Fluid Dynamics |
| DNS | Direct Numerical Solution |
| DTU | Technical University of Denmark |
| EP | Dissipation Rate |
| GCV | General collocated velocity |
| HAD | Hesaplamalı akışkanlar dinamiği |
| IEC | International electrotechnical commission |
| KE | Turbulent kinetic energy |
| LES | Large eddy simulation |
| LIDAR | Light detection and ranging |
| MEASNET | Measurement network of Wind Energy Institutes |
| OMEG | Turbulent frequency |
| PGF | Pressure gradient force |
| PHOENICS | Parabolic Hyperbolic or Elliptic Numerical Integration Code Series |
| RANS | Reynolds Averaged Navier Stokes |
| Re | Reynolds number |
| RNG | Renormalization group theory |
| SODAR | Sound detecting and ranging |
| SRTM | Shuttle Radar Topography Mission |
| SWT | Siemens Wind Turbine |
| WAsP | The Wind Atlas Analysis and the Application Program |
| WRA | Wind resource assessment |
| WTG | Wind Turbine Generator |

# CHAPTER 1

# INTRODUCTION

In the recent years importance of wind energy as renewable and clean energy source increased significantly. Developments in wind turbine technology and increased awareness of the benefits resulted with increased incentives in many countries for using this renewable energy source. As use of wind resources spread widely, importance of having a better understanding for the wind conditions at the sites became more important for where wind projects are planned to be developed.

Use of collected wind data, preparing the appropriate model for the surface conditions, estimating the atmospheric conditions, technical know-how for the use of assessment methodologies and developed programs have crucial importance as all further feasibility studies for the projects are profoundly related with the outcome of wind resource assessment with those inputs. As wind resource assessment is a very early stage process for the projects, wrong interpretation of the collected data, wrong assumptions or high uncertainties in the results may end-up with inappropriate WTG (Wind Turbine Generator) selection –which cannot use the exact potential of the wind at the site-, wrong placing of the WTGs at the site, high maintenance costs or decreased WTG life due to unexpected loads on the WTGs higher than design specifications etc.

For the last 25 years the wind atlas method has been used as an accepted standard resource assessment methodology. For the use of this method, Risø DTU[1] has developed WAsP (The Wind Atlas Analysis and the Application Program) which is currently being used in the wind business excessively. The main factor for the popularity of wind atlas method is the ease of use and understanding of this linear model and the methodology. But with the developments of computation capacities of the computers and programs with improved user interfaces for computing non-linear fluid equations, CFD (Computational Fluid Dynamics) based methods are coming in the limelight. The advantage of CFD based assessment is to be able to create a wind tunnel-like simulation, solve more sophisticated equations and observe conditions those cannot be modeled or captured with linear models, such as separation. Although it is still not

[1] Technical University of Denmark

possible to conclude that CFD approaches give better results, there are many studies showing better validation results compared to conventional linear models, such as the studies of Pereira [1] and Castro[2].

Ayotte [3] noted that despite the broad range of computational methods used in the wind industry they are mainly used for either aeroelastic aspects of wind turbine design or wind resource assessment. The two topics consider different time and length scales and have differences geometrically and topologically. As an example regular grids with finite-difference or finite-volume formulations have been used for meteorological models while irregular grids associated with finite-element codes used for turbine blade design more traditionally but the differences decrease with the development of the meteorological models and higher resolution calculations in more complex geometries. Ayotte gives a brief history about the development of the used methods in common today throughout his study. He also points out the significant effects of turbulent motions on the mean flow when those motions are not represented by the turbulence closure of the used model. In the future some sort of eddy resolving computations are expected to be a part of mainstream calculations of a wind farm design process with the increase of computational power and development of the meteorological modeling.

The errors of the predictions in an assessment can depend on several factors which are well explained in another study of Ayotte [4]. The total modeling error divided into two topics as “Statistical” and “Model Physical” errors. Statistical errors divided further into two as “Data Input Error” which states as the errors in the measurement devices and “Sampling Error” in which errors associated with the duration and frequency of the measurements. Model physical errors have also divided into two sub-topics of “Parameter Space” and “Design” errors. Parameter space error is a result of using a model beyond its limits such as using a linear in a highly complex terrain in which the assumptions of linearization are violated. Design error is the result of the limitations of the model design such as simplifying assumptions which does not take processes or scales into account those exist in the measured flow.

There are still some concerns regarding to complexity of solution of the non-linear equations and more validated results are required for different CFD approaches and site conditions . With this starting point, two different models have been created for the same site by using WAsP and a commercial CFD software WindSim. The error

values of the predicted wind speeds with respect to the measurements calculated and accuracy of both models compared as a validation study of the flow simulations.

A Siemens internal tool has been used in the post-processing phase in order to create time-series by using WindSim model results. This study also aims to validate the post-processing method which has been used to create those synthetic (predicted) time-series. As a first test case for the used post-processing tool a semi-complex site has been preferred where no flow separation was expected. Due to the confidentiality of the used data no detailed information has been given regarding to the site throughout the study.

# CHAPTER 2

# THEORETICAL DESCRIPTIONS AND CONCEPTS

## 2.1. Wind in General

Basically wind is the flow or the movement of the air in large scale. It has plenty of effects to the life on the earth directly or indirectly such as effects on the weather conditions, transportation of the particles in the air or immigration routes etc. For the humankind wind and wind power have also been used for different purposes as well. By inventing the sail boats people were able to travel in further distances or with the basic machinery wind power used for pumping water or graining. With the improvements in the technology today's wind turbines developed and wind power is now used to meet a remarkable amount of the electricity demand.

Before getting to the details and formation of the local and large scaled winds, earth's atmosphere will be explained briefly.

### 2.1.1. Earth's Atmosphere

The Atmosphere is the layer covering the earth and separating the surface from space. Its gaseous envelope mostly consists of nitrogen and oxygen. Water vapor, carbon dioxide and other gases are found as well, but with small amounts when compared. Atmosphere can reach up to hundreds of kilometers above the ground, but almost 99 % of its atmosphere lies within approximately 30 km from the surface. As atmosphere is eventually merging with empty space, becoming thinner in time and has different thickness at different parts of the earth there is no definite upper limit can be defined. [5]

In the vertical profile of the atmosphere, regions with different properties are existing. Those regions are divided into several layers by considering changes of properties such as air temperature variation, gases compromised or even electrical properties [5]. The main layers and heights above the surface are as shown in the figure below and explained here briefly;

**Trophosphere:** This layer is the closest to the earth's surface where weather occurs and life forms. Atmospheric Boundary Layer (ABL), where the wind conditions that will be assessed in this study takes place, is the lowest part of this layer and will also be explained in more detail.

**Stratosphere:** It is the layer above tropheosphere and temperature rises with height.

**Mesosphere:** Due to low density air in this layer is very thin and molecules are great distances apart. Stratosphere and mesosphere are also known as the middle atmosphere.

**Thermosphere:** This is the layer which is also known as upper atmosphere. Temperature also rises with height but as the air molecules are too far apart it is not possible to measure the temperature with a thermometer, but by looking at the motion and speed of the rarefied gases. The temperature would reach to thousands of Celsius degrees.

The approximate temperature relation with height is also shown in the following figure (eg. For Trophosphere 0.65 K/100 m), which may vary with changes in physical conditions. Additionally, beside the mentioned layers here **exosphere** exists above thermosphere, which has very few atmospheric molecules those can escape into space. This layer is not shown in the layers figure below.

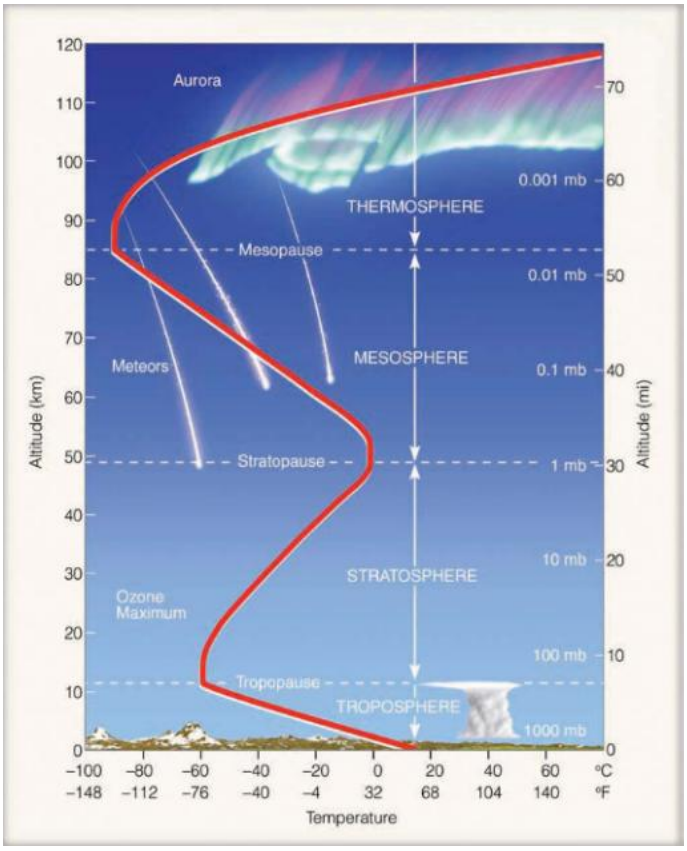


Figure 2.1. Average temperature above the ground and layers of the atmosphere [5].

### 2.1.2. Global and Local Winds

The wind occurs because of the pressure differences of two different regions. Due to the difference air tends to move from the high pressure to low pressure regions. Those pressure differences occur because of uneven absorption of the solar radiation of the earth's surface.

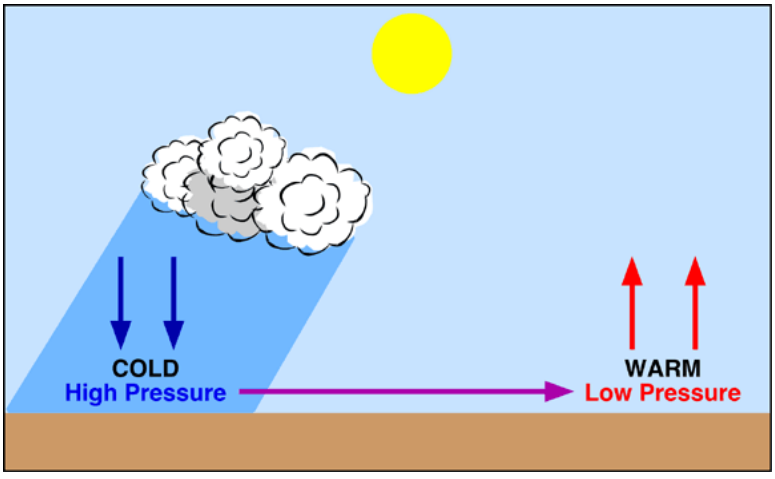


Figure 2.2. Wind flow from the high to the low pressure region. [6]

From the basic knowledge of wind flow from cold to warmer regions –or high pressure to low pressure- George Hadley (1685-1768) carried out a discussion regarding to the global winds in 1700's. What Hadley had proposed was a single-cell circulation pattern which is shown in the below figure.

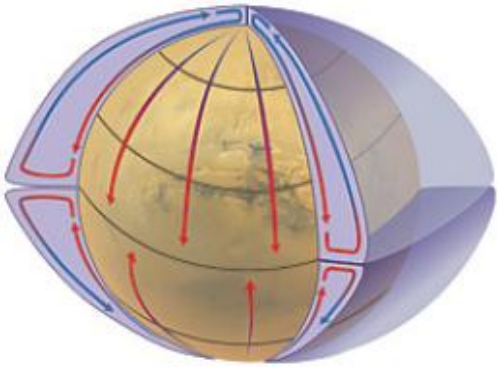

Figure 2.3. Hadley's single-cell circulation pattern from 1700's. [7]

Since the earth's axis is titled, it rotates and land-sea ratios differ in the northern and southern hemispheres the actual pattern is much more complicated. Although it is still too much simplified global Three Cell Circulation Pattern can be used to explain global winds. The pattern is shown in figure below.

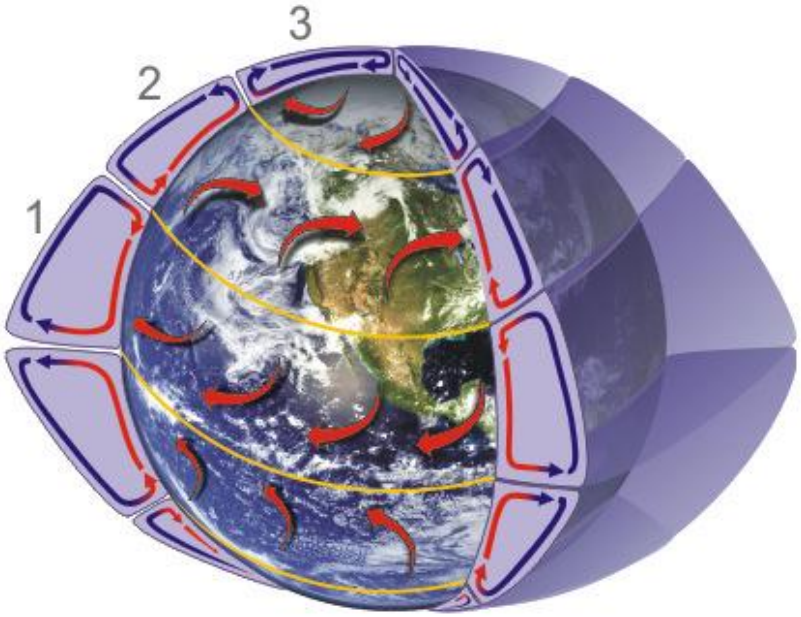


Figure 2.4. Simplified Global Three Cell Surface and Upper Air Circulation Patterns. [7]

The three circulations in the atmosphere are as below:

1. Hadley Cell: Air moves toward the equator and heats up during this movement. Due to increased temperature it moves vertically around the equator and moves toward the poles in the upper atmosphere. The winds in this cell are called as “Trade Winds”.
2. Ferrel Cell: In this cell the air flows pole-ward in the low-attitude and towards equator in the upper atmosphere. The winds in this cell are called as “Westerlies”.
3. Polar Cell: Air moves again towards the equator in the lower altitude as in Hadley Cell and to the poles in the higher altitudes. As the air gets cooler and shrinks it sinks near the poles and causes polar highs. The winds in this cell are called as “Polar Easterlies”.

As can be seen from the figure the wind direction shifts to the right of the flow direction which is caused by the rotation of the earth, in other words the Coriolis phenomenon which will also be explained under Atmospheric Boundary Layer topic.

Atmospheric motion has been investigated by categorizing different phenomena according to their spatial and temporal scales.

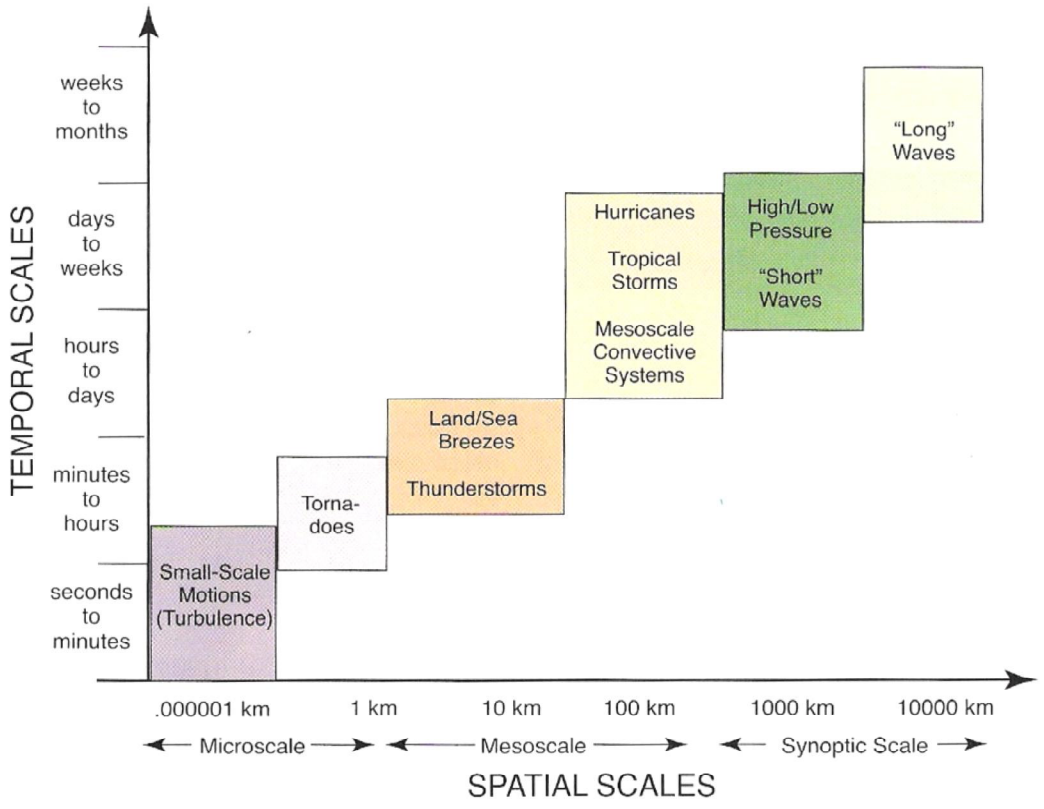


Figure 2.5. The spatial and temporal scales of various weather phenomena. [8]

Influence of the geographic features on the flow increase as the temporal and spatial scales get smaller. The resulting pressure differences from tens to couple of hundred kilometers cause the local winds. Local winds named differently over the globe and show various characteristics.


Figure 2.6. Local winds around the world. [9]

The main local winds can be summarized as;

**Sea Breezes:** During the day high pressure is created over the sea while low pressure occurs over the land due to uneven heating. This cause a the air to move from sea to the land.

**Land Breezes:** In contrast to the sea breezes, during the night low pressure over the sea and high pressure over the land causes the air to move from the land to the sea.

**Mountain Breezes (Anabatic Winds):** Similar to the process of land and sea breezes, mountain breezes occur due to uneven heating of valley and mountain top. During the day time sun heats up the valley air, causes it to rise and creates an up-slope wind.

**Valley Breeze (Katabatic Winds):** During the night the air on top of the mountain cools more rapidly and moves to the lower elevated valley as a down-slope wind.

## 2.2. Atmospheric Boundary Layer (ABL)

Atmospheric Boundary Layer, which is also known as Planetary Boundary Layer (PBL), is the lowest part of the Troposphere where different weather events take

place, is inhabitable part of the atmosphere and the region of interest for this study [10]. According to Stull [13] its behavior is directly influenced by the interaction with the planetary surface. Those planetary surface effects are mainly caused by the friction and heat fluxes at the ground. As Stull stated in this study; "that part of the atmosphere that is directly influenced by the presence of the earth's surface, and responds to surface forcings with a timescale of about an hour or less".

The height of ABL may vary between one hundred meters and a few kilometers which is very difficult to define the exact height as it depends on the time of day, exact weather conditions and surface effects. With certain assumptions such as neutral stability condition (where the heat flux in the vertical direction is negligible) the ABL can be divided into several sublayers.

**Canopy Layer:** It is the layer covering the surface, where the obstacles are found. Coriolis forces' effects are negligible.

**Surface Layer:** Above canopy layer, where Coriolis forces can also be neglected and the flow is turbulent.

**Ekman Layer:** Above surface layer. As moved up in that layer effects of the surface friction decrease while the Coriolis forces become more dominant.

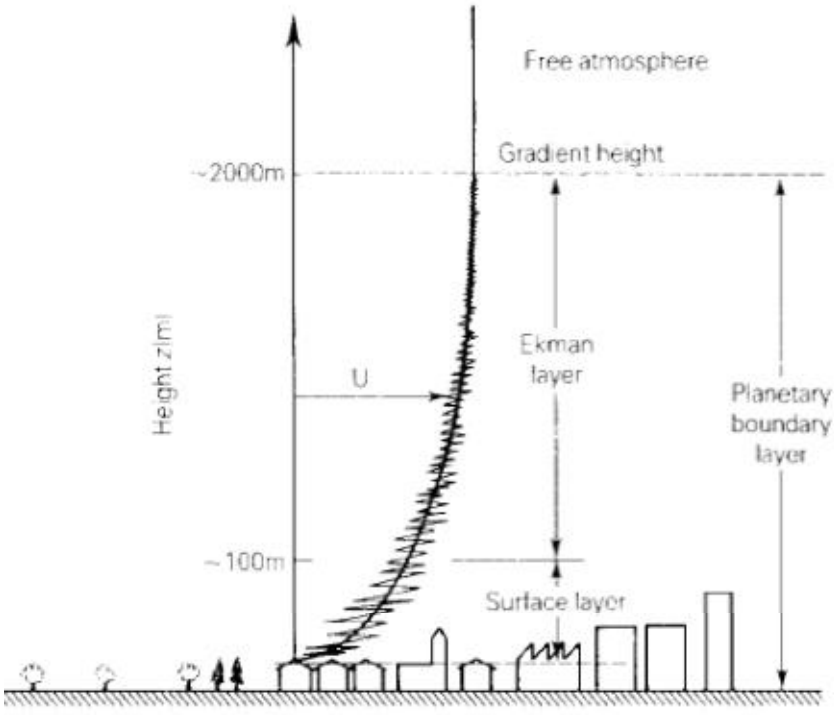


Figure 2.7. The sublayers of the ABL in a neutral atmospheric condition. [11]

By moving upward in the atmosphere the increased wind speed and as a result effect of the Coriolis Force the direction of the flow changes gradually.

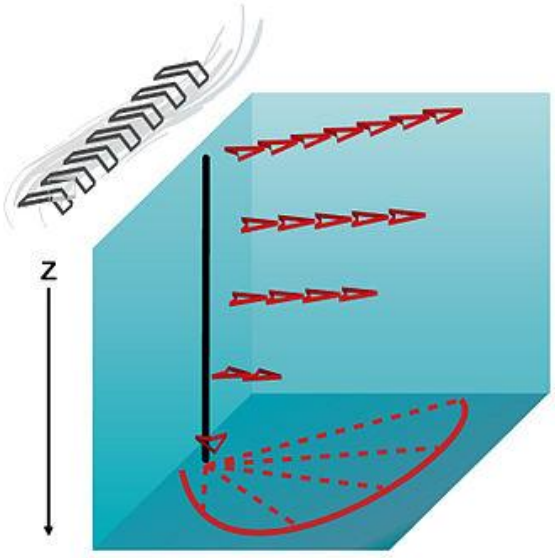


Figure 2.8. The change in the wind direction in the Ekman Layer. [12]

Geostrophic Winds are the winds occur above the ABL. Basically those winds are affected by the friction of the surface in a negligible amount. The change of direction of the wind in the upper heights, is also shown in the below figure. At the point 1 the air parcel is only driven by Pressure Gradient Force (PGF) which causes the air to move from high pressure to low pressure region. As the air begins to move the Coriolis Force (CF) deflects the air to the right. As the wind speed increases in points 2,3 and 4 coriolis force affecting the parcel also increases. The wind speed increases until the Pressure Gradient Force and the Coriolis Force balanced (Point 5). Here the Geostophic Winds parallel to the isobars forms.

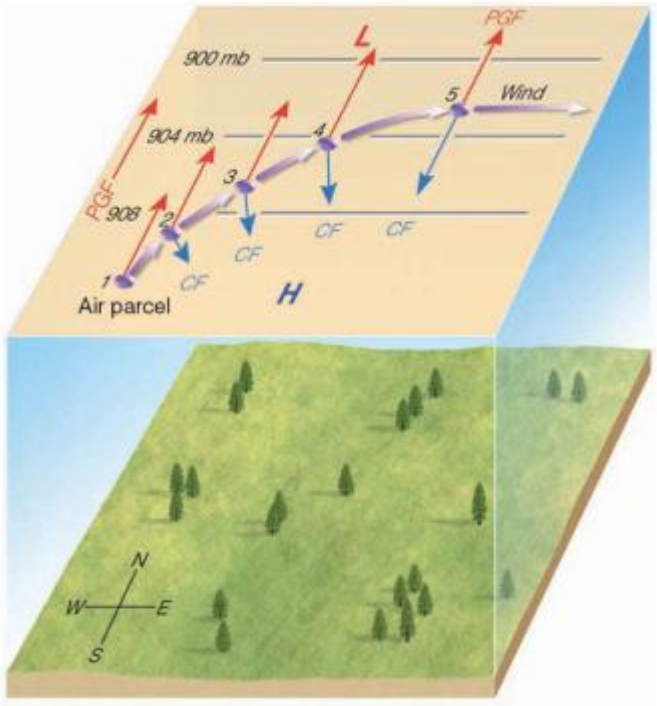


Figure 2.9. Increase of the CF in the Ekman layer until balanced with the PGF [5]

### 2.2.1. Stability Conditions

In the lower parts of the ABL, wind profile (therefore ABL height) is mainly characterized by the thermal stability conditions and roughness of the site. Thermal stability is the property that describes the behavior of temperature in an arbitrary parcel of air, independent of the pressure by means of the potential temperature [13]. It is divided into three different conditions such as “neutral”, “stable” and “unstable”.

For a better explanation of the stable atmospheric condition, taking a meteorological balloon into an account as a parcel of air would be useful. The balloon consists of air at the same temperature and pressure levels with the environment at the ground position. When it is lifted in the air, in an adiabatic condition (where no heat transfer occurs between the environment and the balloon), due to decrease in pressure and increase of the volume, temperature will drop for the parcel of air. The change of temperature inside the balloon is called as “adiabatic lapse rate”. If the “environmental lapse rate” is lower than the “adiabatic lapse rate” inside the parcel, the temperature of the air in the balloon will be lower, the density and weight will be higher than outside. This will result the balloon to tend to return its initial position –to the ground- and the condition for the air parcel called as “stable”. In the other way round, in unstable condition, environmental lapse rate is higher than the adiabatic lapse rate and parcel of

air tends to rise. When those two lapse rates are equal, the condition is referred as "neutral", in which the parcel of air stays in balance without any tendency to sink or lift [5].

In the same manner as already stated, for neutral conditions air parcel is expected to keep its position above the ground and follows the hill in the flow direction. In stable conditions rise of the air is prevented due to blocking effects caused by the upper layer of the atmosphere. For that reason air follows a path around the hill rather than uphill, with a minimal change in the height of the flow. In unstable conditions, with the buoyancy effect, rising air in the uphill direction does not follow the trajectory in the downhill direction, but keeps rising. Figures for three different conditions are shown below.

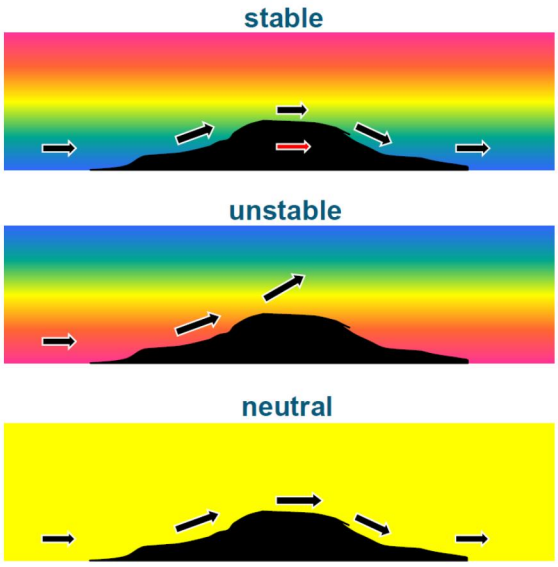


Figure 2.10. Wind behavior in different atmospheric stability conditions [14]

Potential temperature change with height is an indicator for the stability condition of the site. In neutral stability condition potential temperature does not change with height and constant. While potential temperature decreases with height in thermal instability case, it increases in stable conditions. As stated above, atmospheric stability conditions have significant effects on the wind profile due to exchange of momentum over height. Difference of the profiles as shown in figure below. There are several other methods to estimate the stability condition at the site as analyzed by Mohan and Siddiqui [15].

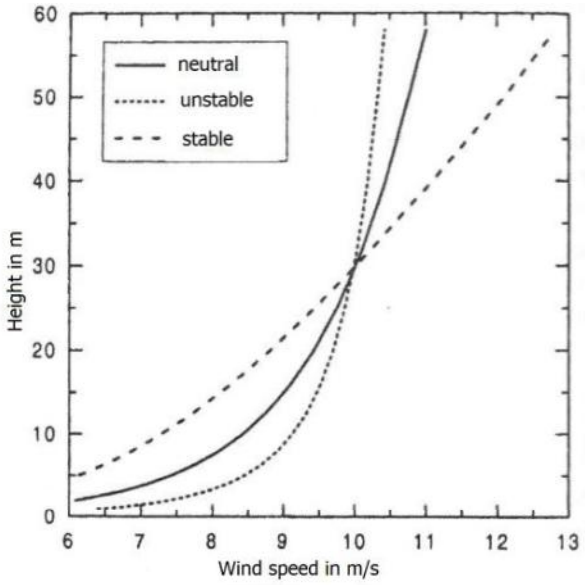


Figure 2.11. Change of wind shear with respect to stability condition. [16]

In stable conditions higher wind shear expected due to lower buoyancy effects on the flow. Buoyancy effects decreases the change of wind speed with height while increasing turbulence in the flow, as in unstable wind conditions, resulting with a lower shear and higher turbulence.

### 2.2.2. Vertical Wind Profile

The variation of wind speeds with height has been explained with several mathematical models with some assumptions. In the neutral atmospheric conditions, when the thermal effects are negligible and basic models such as "The Log-Law" and "The Power Law" are the most common ones, also actively used for the site assessment. In the stated equation for the Log-Law (1.1) roughness properties of the terrain need to be defined. Here, roughness length $z_0$ can be considered as the height, where the wind speed is zero. The roughness classification for the terrain types has been done in European Wind Atlas [17] and used for the wind assessments as a standard. U(z) is the mean wind speed at the height of interest"z", $\kappa$ is Von Karman constant ($\approx 0.4$), $u_*$ is the friction velocity, $\tau_{wall}$ is the shear stress and $\rho$ is the air density.

$$U(z) = \frac{u_*}{\kappa} ln\left(\frac{z}{z_0}\right) \tag{2.1}$$

$$u_* = \sqrt{\frac{\tau_{wall}}{\rho}} \tag{2.2}$$

Friction velocity is dependent on the nature of the surface and magnitude of the wind and has emerged as an important scaling parameter in surface layer studies.[10]

In non-neutral atmospheric conditions a new empirical function of $\Psi$ introduced to the equation (2.1) as:

$$U(z) = \frac{u_*}{\kappa}\left[\ln\left(\frac{z}{z_0}\right) - \Psi\left(\frac{z}{L}\right)\right] \tag{2.3}$$

L is called as "Monin-Obukhov lenght" which leads the function of $\Psi$ to become dimensionless. $\Psi$ function depends of stability of the atmosphere and it is negative for unstable conditions and positive for stable conditions. [18]

The equation of the other well know method – Power Law- is shown in (2.4):

$$\frac{U_1}{U_2} = \left(\frac{z_1}{z_2}\right)^{\alpha} \tag{2.4}$$

The experimentally defined „α" is the wind shear exponent which the profile depends on for the power law, $U_1$ and $U_2$ are simultaneous steady wind speeds over terrain levels of $z_1$ and $z_2$ respectively. Despite the over simplicity of the wind shear exponents and insufficiency for stability conditions other than neutral, it is still used when approximate estimations are required.

## 2.3. Site Assessment

The site assessment is the process of investigating the site conditions with the collected data and information. In the scope of wind farm investments and developments, the findings of the assessment may be used in various studies. A proper estimation of annual energy production (AEP), choosing right places for WTGs or choosing suitable WTG type can be done with correct interpretation of the collected data. Site assessment is a crucial step in the wind projects as the life of the turbine and profitability of the projects is highly related to.

### 2.3.1. Measurements

In order to have a better understanding of the wind conditions of the site proper measurements are required. For that reason measurement masts (also used as "met masts" or "masts") need to be installed to the locations those assumed to be representative for the areas of interest, in other words possible WTG positions. Here representativeness can basically be expressed as the similarity of the surface and wind conditions around the position of mast and position that the flow conditions to be assessed. The representativeness is also related to the complexity of the site. As an example for sites with flat terrain the representative distances are much more than the complex sites with hilly terrain. To determine the complexity and the representativeness of the measurement locations the recommendations by IEC [19] and MEASNET [20] would be useful. But the recommendations are generalized and not possible to cover every case. Therefore the experience of the siting engineer becomes even more important while analyzing the assessment results.

The essentially required measurement sensors, devices and specifications for a proper measurement campaign are explained by MEASNET [20]. Briefly, following measurement sensors and devices are required;

**Anemometer:** Used for the wind speed measurements. Cup anemometers which measures the horizontal wind speeds are used for most of the measurement campaigns. All anemometers to be installed on a met mast must be calibrated according to the MEASNET guideline [21] by a MEASNET approved institute. In order to observe the change of wind speed in the vertical direction at least two anemometers required on the met mast. Anemometers capable of measuring the vertical component of the flow (such as vertical anemometers) are also preferred to be used.

**Wind Vane:** Used to measure the direction of the wind. More than one wind vane is preferable for further comparison and increase the data availability in case of any failures of the sensors during the measurement campaign.

**Temperature, Humidity and Pressure Sensors:** The data can be used for the calculation of the air density, mean, minimum and maximum values for the measurements etc. which are used to decide the suitable WTG type with the appropriate specifications and settings.

**Data Logger:** All sensors are connected to the loggers which are also located on the met mast in order to monitor and store the collected data.

Installation of the met mast, orientation of the booms and sensors are also crucial in order to minimize the disturbances caused by the mast and other sensors. As even small disturbances in the flow and measurements may lead to medium to high uncertainties in the assessment results the recommendations for the mast and sensor installations given in IEC 61400-12-1 [22] must be followed.

Beside measurements with traditional met masts, in the recent years newer measurement methods such as LIDAR and SODAR [23] are also being used more frequently, especially for the sites where wind conditions in greater heights (more than 100m a.g.l) are interested.

### 2.3.2. Modeling the Site

Before running the calculations several inputs are required to create the model of the wind farm. Following data and information are required to create the model;

**Time Series Data:** Data collected from measurement masts which are representative for the site area. The data averaged to 10 minutes and basically include measured parameters such as mean wind speed, turbulence intensity, wind direction and temperature. Those parameters are preferred to be measured from more than one height for investigating the dependence of the wind conditions to the height above ground. There are many other parameters such as upflow wind speeds, pressure, humidity, etc. which is a matter of decision to measure or not regarding to detail or purpose of the planned assessment.

**Elevation Data:** The flow over the surface is highly affected by the surface conditions. Change in the height and shape of the surface adds local effects on the flow such as speed-ups, speed-downs and change in direction. The effects of height variations have been investigated with an international field experiment at the Askervein hill on the Isle of South Uist in the Hebrides [24]. In order to simulate the flow or calculate the orographic effects (which are caused by elevation changes), proper data of the elevation must be added somehow to the prepared model. For the assessment process, digitally prepared contour lines (also known as isolines) are used as another

input for the model. Those maps either can be prepared by topographers or used directly from available databases such as Shuttle Radar Topography Mission (SRTM)[2].

**Roughness Data:** The roughness of the assessed site is another surface property that affects the flow over the surface. The vegetation type such as forests, meadows, bushes etc. or differences caused by land or water are affecting the flow in different ways. As the height and density of the roughness element increase, friction effect on the flow also increases, resulting as lower wind speeds or higher wind shears.

The roughness length is a useful parameter to define and understand the roughness classification. When the Log-Law is used for the wind profile estimation, the roughness length, $z_0$, is the height above ground where the mean wind speed becomes zero. For the certain surface types, the European Wind Atlas [17] includes a detailed explanation of the used computational methods in order to determine the roughness length as an input for the model.

**Obstacles:** Obstacles are the objects causing sheltering effects and decreasing the wind speed behind. Whether an obstacle provides shelter at the specific site depends upon the followings [17]:

- the distance from the obstacle to the site
- the height of the obstacle
- the height of the point of interest at the site
- the length of the obstacle
- the porosity of the obstacle

### 2.3.3. Climatic Conditions and Design Specifications

With the collection of stated data, the model of the site to be assessed ready to be prepared. The collected data can be combined in various commercial assessment programs, which two of them with different approaches will be explained extensively in the following chapters. The conditions to be assessed are followed below [17]:

**Normal Wind Conditions:** Mean wind speed, sector-wise Weibull parameters, turbulence intensities, wind shear exponent and flow inclination are the conditions to be assessed in a general wind assessment procedure.

[2] A more detailed information is available in http://www2.jpl.nasa.gov/srtm/

**Extreme Wind Conditions:** For the structural integrity of the WTGs possible 10 minute mean wind speed ($V_{ref}$) and 3 seconds gust wind speed ($V_{e50}$) with a recurrence period of 50 years have to be calculated with various statistical methods.

**Other Environmental Conditions:** Temperature, humidity, air density, seismic activities, soil class, salinity are some of the environmental conditions which need to be assessed or checked in order to avoid any future risks. Those parameters have to be within certain limits in order to avoid issues such as icing on the blades (caused by low temperature and high humidity), cooling system error and low energy yields (caused by low air density), increased loads on WTGs (caused by high air density), extreme loading on the WTGs resulting with structural integrity issues (caused by seismic activities).

For the classification of the WTGs according to the design loads IEC [19] provides a comprehensive guide. According to the normal and extreme wind conditions IEC classifies the WTGs as stated in the following table;

Table 2.1. Basic parameters for WTG classes [19]

| Wind turbine class | | I | II | III | S |
|---|---|---|---|---|---|
| $V_{ref}$ | (m/s) | 50 | 42,5 | 37,5 | Values |
| A | $I_{ref}$ (-) | 0,16 | | | specified |
| B | $I_{ref}$ (-) | 0,14 | | | by the |
| C | $I_{ref}$ (-) | 0,12 | | | designer |

where,

$V_{ref}$ is the reference wind speed average over 10 min,

A designated parameter for higher turbulence characteristics,

B designates the category for medium turbulence characteristics,

C designates the category for lower turbulence characteristics,

$I_{ref}$ is expected value of the turbulence intensity (Mean value) at 15 m/s.

The 3 seconds gust $V_{e50}$ value also important while defining the WTG class. By using $V_{ref}$, $V_{e50}$ can easily be calculated with the following formula,

$$V_{e50}(z) = 1.4V_{ref}\left(\frac{z}{z_{hub}}\right)^{0.11} \quad (2.5)$$

Where z is the height of the measurement and $z_{hub}$ is the hub height of the assessed WTG type. When the formulation applied to the $V_{ref}$ values in the above table resulting $V_{e50}$ values are 70, 59.5, 52.5 m/s for classes of I, II, III respectively.

# CHAPTER 3

# METHODOLOGY

## 3.1. Linear Approach

WAsP (The Wind Atlas Analysis and the Application Program) is a tool used for vertical and horizontal extrapolation of the wind climate statistics. This software contains several models for wind flows over different terrain and close to sheltering objects. Conceptually the WAsP methodology consists of five main calculation blocks which are explained briefly below for a better understanding of the general use of the tool. [25]

**Analysis of raw wind data**. In order to assess the site conditions data from a source that is considered to be representative for the wind farm site is required. This required data can either be from an onsite measurement or a local meteorological station measurements. With the available time-series data a statistical summary of the observed, site specific climate can be provided.

**Generation of wind atlas data**. After analyzing the data, the program is able to convert the data into a regional wind climate or wind atlas data set. The wind observations or measurements can be called as "cleaned" in a wind atlas data set with respect to the site specific conditions which are the roughness, orographic and shelter effects. Therefore the wind atlas data sets become site-independent and the wind distributions have been reduced to certain standard conditions. Due to this similarity of the created data sets with the geostrophic wind, they can be also called as quasi-geostrophic.

**Wind climate estimation**. By using the calculated wind atlas data set (which can be either calculated by WAsP or obtained from another source such as the European Wind Atlas [17]) the wind climate at any specific position or height of the site can be estimated. Here the inverse of the generation of wind atlas calculation is used. By introducing descriptions of the terrain (roughness, orographic and shelter effects) around the predicted site, the models can predict the actual, expected wind climate at

this site. This transformation of measured wind data to the positions in interest which is stated until now is also shown in figure below:

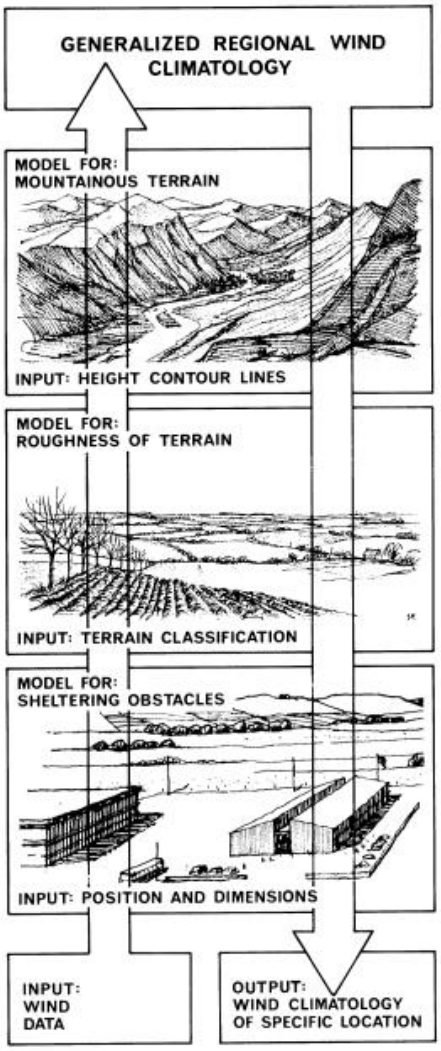


Figure 3.1. Wind Atlas Methodology [17]

The definition of the site-specific conditions is crucial here as the assessment results are highly dependent on those descriptions. First making the distinction between a roughness element and an obstacle is important as they are implemented differently in the model. As already mentioned in section 2.3.3 the decision of using a roughness element or objects as an obstacle in the model depends of several conditions. If the point of interest (anemometer or wind turbine hub) is closer than about 50 obstacle heights to the obstacle and closer than about three obstacle heights to the ground, the object should probably be included as an obstacle. In this case the obstacle should not at the same time be considered as a roughness element. If the point of interest is further

away than about 50 obstacle heights or higher than about three obstacle height, the object should most likely be included in the roughness description [25].

In order to calculate the wind conditions at a certain point in the model the effects of roughness and orography is taken into account with a weighting of the distance. As expected in the real conditions the effects of the elevation differences and roughness decrease with the increase of distance from the position of interest. Therefore the effects are also weighted in a same manner. As considering the point of interest in the center of the model, the minimum suggested height contours and roughness areas are 5 and 10 km respectively [25]. But to decrease the uncertainties in the results of the assessments, 10 km for height contours area and 20 km roughness are preferred.

**Estimation of wind power potential**. In the further steps of the assessment, calculated wind conditions can be used for the estimation of the wind power potential of the site. In order to calculate the potential a WTG type should be specified. As each WTG has its own power productions in different wind speeds, the power curve of the WTG in question is also required. By using those two information wind power potential can be calculated.

**Calculation of wind farm production**. As the wind passes through the sweeping area of the WTG blades the flow becomes disturbed and changes in its velocity occur. The deficit in the velocity of the flow is implemented into the model with two parameters which are the $C_t$ curve and wake decay constant. $C_t$ is the coefficient of the turbine at a specific wind speed and $C_t$ curve for each WTG is needed for the operating wind speeds. The other parameter, wake decay constant is basically the rate of expansion (or break-down) of the wake.

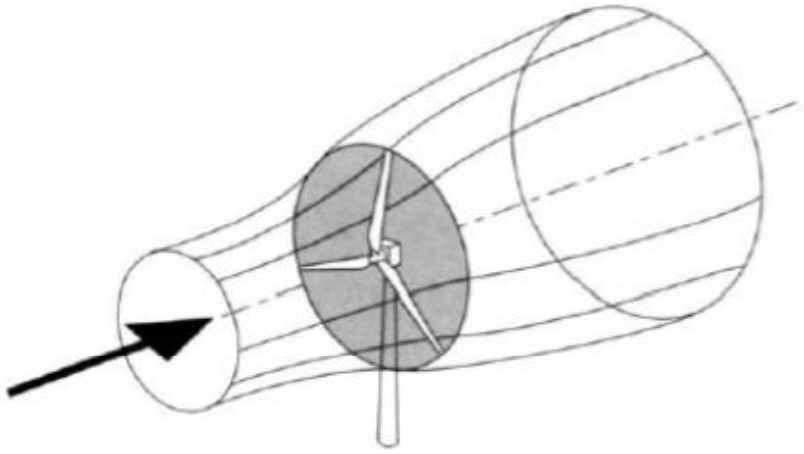

Figure 3.2. The deficit of the flow passing through the sweep area [18]

With those given thrust coefficient curve of the WTG, wake decay constant and the wind farm layout WAsP can calculate the losses caused by the disturbance of the wind for each WTG in the layout. Calculation of the wake losses allows the reach the net energy production of the wind farm by subtracting those losses from the gross energy production. The main purpose of this thesis is to investigate the modeled wind conditions with respect to linear and CFD approaches at a specified location. In this study wake effects have been ignored and gross energy productions have been compared.

## 3.2. CFD Approach

In addition to the linear wind farm area modeling methods -such as WAsP- in the recent years solution of non-linear Navier Stokes Equations with an advanced numeric processing has also been used more frequently with the help of several commercial software. WindSim (a user interface for the CFD software PHOENICS) is one of those widely used commercial programs which also used for this comparison study.

With its PHOENICS solver WindSim models the flow field by using Reynolds Averaged Navier Stokes (RANS) equations. The approach of RANS is a time-averaged solution and differs from other CFD techniques with time-step approach such as Direct Numerical Simulation (DNS), Large Eddy Simulation (LES) and Detached Eddy Simulation [26]. The model solves the atmospheric flow for a "steady-state" case for a chosen wind direction. By "steady-state" it is meant that the time derivative in the RANS equation is forced to be zero. By simulating for several different wind directions (sectors) an annual average wind speed can be generated. The models are run for a given set of constructed boundary and initial conditions [27].

By using the RANS equation it is not possible to calculate the eddies in the flow as the method uses a time averaging process on the Navier Stokes equation. Although this process decreases the accuracy of the method when compared to DNS or LES, it also decreases the computational demand and becomes suitable for practical use. The processes for DNS, LES and RANS equations can be shown as below;

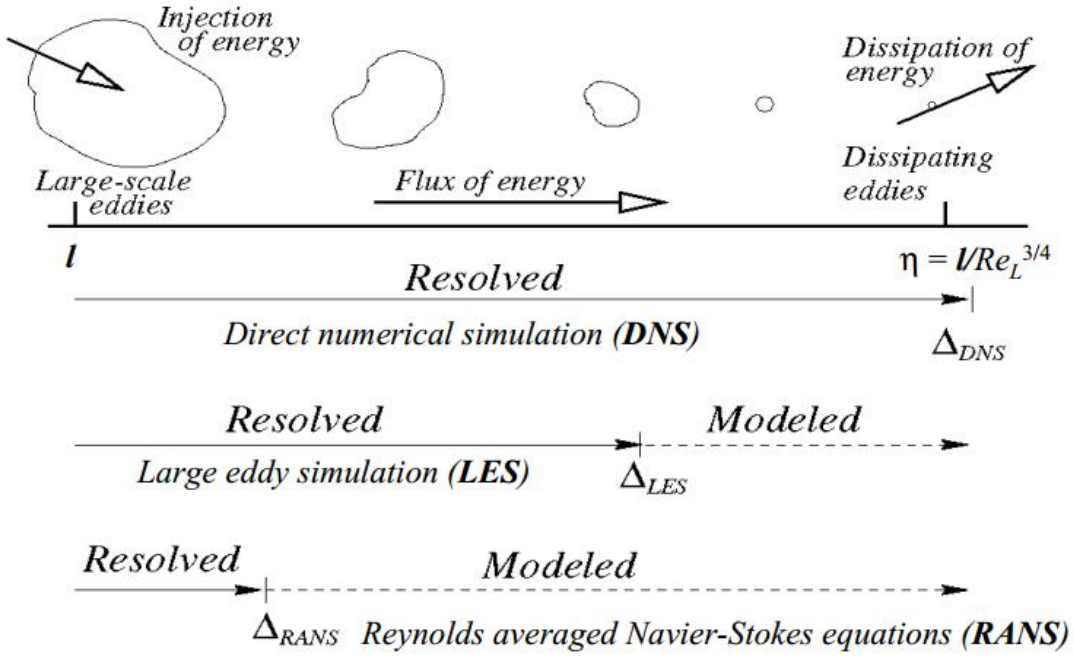


Figure 3.3. Processes for DNS, LES and RANS [28]

With the averaging the conservation of mass and momentum equations take the below form:

Conservation of mass:

$$\frac{\partial \rho}{\partial t} + \frac{\partial u_i}{\partial x_i} = 0 \tag{4.1}$$

For an incompressible fluid (where the density is constant):

$$\frac{\partial u_i}{\partial x_i} = 0 \tag{4.2}$$

Conservation of momentum:

$$\rho \frac{Du_i}{Dt} = \frac{\partial(\rho+\tau_{ii})}{\partial x_i} + \frac{\partial \tau_{ji}}{\partial x_j} + \frac{\partial \tau_{ki}}{\partial x_k} \tag{4.3}$$

Three linear elongating deformation components:

$$e_{ii} = \frac{\partial u_i}{\partial x_i} \tag{4.4}$$

Six shearing linear deformation components:

$$e_{ij} = e_{ji} = \frac{1}{2}\left(\frac{\partial u_i}{\partial x_j} + \frac{\partial u_j}{\partial x_i}\right) \tag{4.5}$$

The volumetric deformation:

$$\frac{\partial u_i}{\partial x_i} \tag{4.6}$$

Rates of deformation are proportional with the viscous stresses in a Newtonian fluid. Therefore the viscous stress components can be written as:

$$\tau_{ii} = 2\mu\frac{\partial u_i}{\partial x_i} + \lambda\frac{\partial u_i}{\partial x_i} \tag{4.7}$$

$$\tau_{ij} = \tau_{ji} = \mu\left(\frac{\partial u_i}{\partial x_j} + \frac{\partial u_j}{\partial x_i}\right) \tag{4.8}$$

By applying (4.7) and (4.8) to (4.3) Navier-Stokes equation can be derived. The compact form of the equation is given as below:

$$\rho\frac{\partial U_i}{\partial t} + \rho u_j\frac{\partial u_i}{\partial x_j} = -\frac{\partial P}{\partial x_i} + \frac{\partial}{\partial x_j}(2\mu e_{ij} - \rho\overline{u_i' u_{J\iota}'}) \tag{4.9}$$

where,

| | |
|---|---|
| $U_i$, Uj | mean velocity (m/s) |
| $x_i$, $x_j$, $x_k$ | position vector |
| t | time (s) |
| P | mean static pressure ($N/m^2$) |
| ρ | density ($kg/m^3$) |

| | |
|---|---|
| $\mu$ | first (dynamic) viscosity (kg/s*m) |
| $\lambda$ | second viscosity (kg/s*m) |
| $\tau$ | stress component (Pa) |
| $u_i', u_{ji}'$ | fluctuating velocity (m/s) |

Current study deals with a domain area with a couple of kilometers in dimensions and neutral stability condition in the ABL. Therefore in these kinds of flows compressibility and thermal effects can be neglected [29] and the solution of energy equation is not needed.

In the stress tensor turbulent fluctuations of the flow appear in RANS equations which cause a closure problem. In order to close the system several turbulence models can be used. The turbulence models those can be used for closing the system are k- ε and k- ω , which WindSim also uses. Additionally there are several k- ε models with some modifications that WindSim uses such as;

- Modified k- ε model,
- k- ε with YAP correction,
- RNG k-ε model.

Although the used turbulence model has significant effects on the resulting wind speeds –especially in complex sites where flow separation phenomena occurs- comparison for the turbulence values and turbulence models are not included in this thesis. Using other turbulence models and a sensitivity analysis regarding to the comparison of the results can be noted down as a possible further improvement.

# CHAPTER 4

# INPUT DATA AND MODEL SETTINGS

The estimated wind conditions are highly dependent on the input for the model as well as the used flow model and settings. Therefore the quality of the used elevation information, roughness description, uncertainty in the measurements and model settings are crucial which have been described below.

## 4.1. Orography

The flow conditions are affected more by the surroundings of the masts' and positions to be assessed. As the distance from those locations increase the effects from the elevation differences decrease gradually. Due to that reason a large scale elevation map with the scale of 1:1000 has been used for the site area. As the used scale is large small elevation changes down to 1m are can be captured by the map.

Those 1:1000 scale maps are generally prepared for special purposes and expensive. For wind projects those maps are usually prepared for the site area which can extent to several kilometer distances from the planned turbine positions. Therefore only using those large scale maps is not sufficient for wind assessment purposes as the flow conditions can be affected with the elevation changes in greater distances. To cover larger distances 1:1000 scale maps can be merged with less detailed maps are easier to obtain and with sufficient accuracy. For the current site 1:25000 scale map has been cut and merged with 1:1000. The combined map which can be seen in below figure has been used for the further assessment process. The upper parts of the all maps shown below are north.

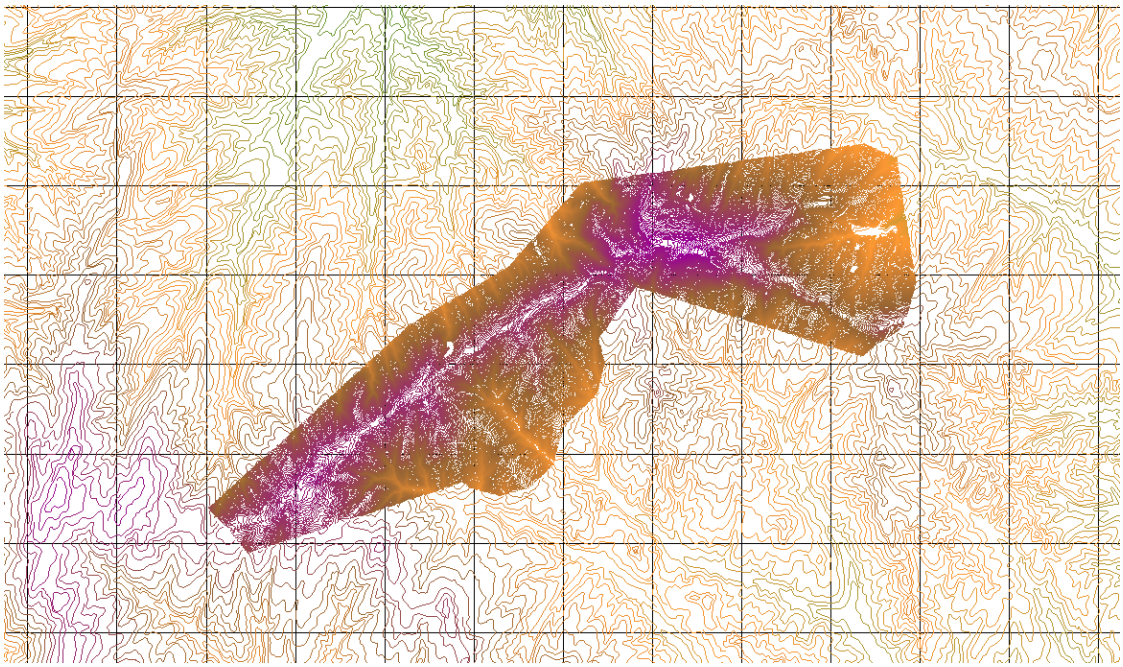

Figure 4.1. Merged elevation map.

As can be noticed the site area in the middle of the map is darker as 1:1000 scale map contains isolines for every 1 meter elevation difference while isolines for 1:25000 maps are drawn for every 10 meters. The lines can be seen in detail with further zoom which is also shown below:

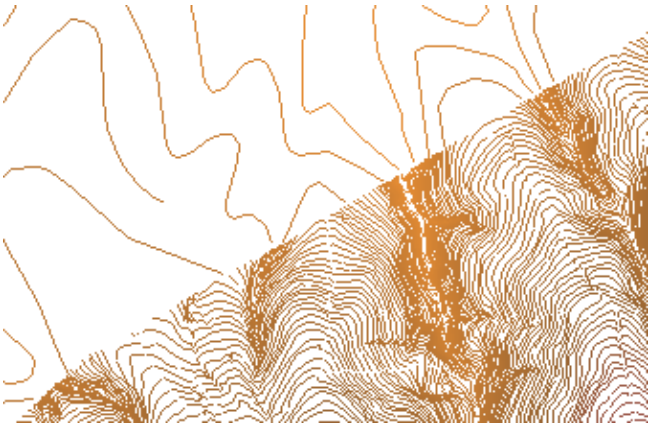

Figure 4.2. 1 and 10 meter isolines from merged elevation map

## 4.2. Roughness

In order to prepare sufficient model roughness maps of at least 100xhub height or 10x10 km area around the mast and WTG locations is recommended in the WAsP best practices and checklist [30]. In order to fulfill that recommendation approximately 20x20 km roughness map used in the model. Rather than creating a roughness map manually for such a large area Corine Land Cover (also known as CLC) data has been used. CLC data only include land use cartography with descriptions of land occupation and features with an original scale of 1:100,000. The roughness length information is not included in the database therefore the classification suggestions from Silva, Riberio and Guedes [31] used for the modeling.

Similar to orographic effects, roughness effects are also weighted with distance to the location of interests. This increases the importance of the details in the vicinity of the site area. Although the details of the CLC data is adequate for greater distances, site area and the vicinity has been modified manually with more details. For the modification process available on-site and satellite photos have been used.

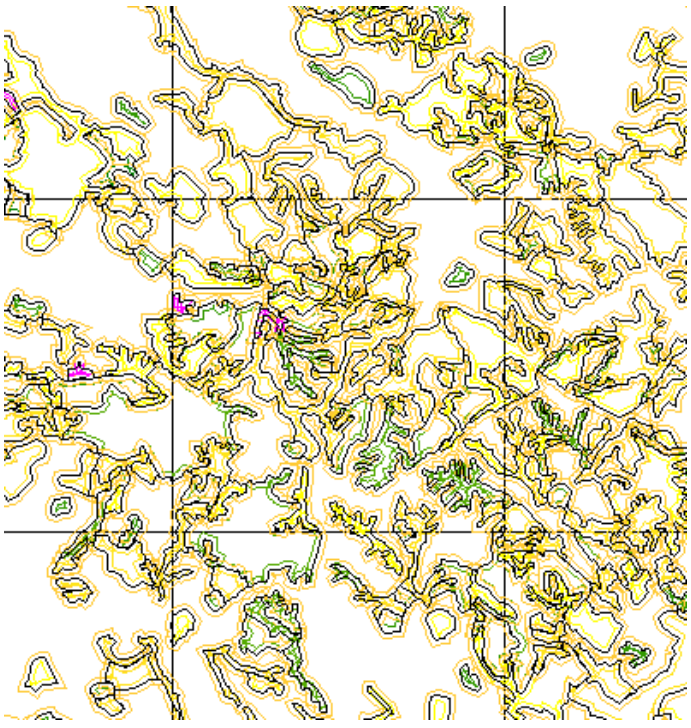

Figure 4.3. From the roughness map used for the assessment

## 4.3. Measurements

For the assessment three met masts have been used and positions on the elevation map are as shown below.

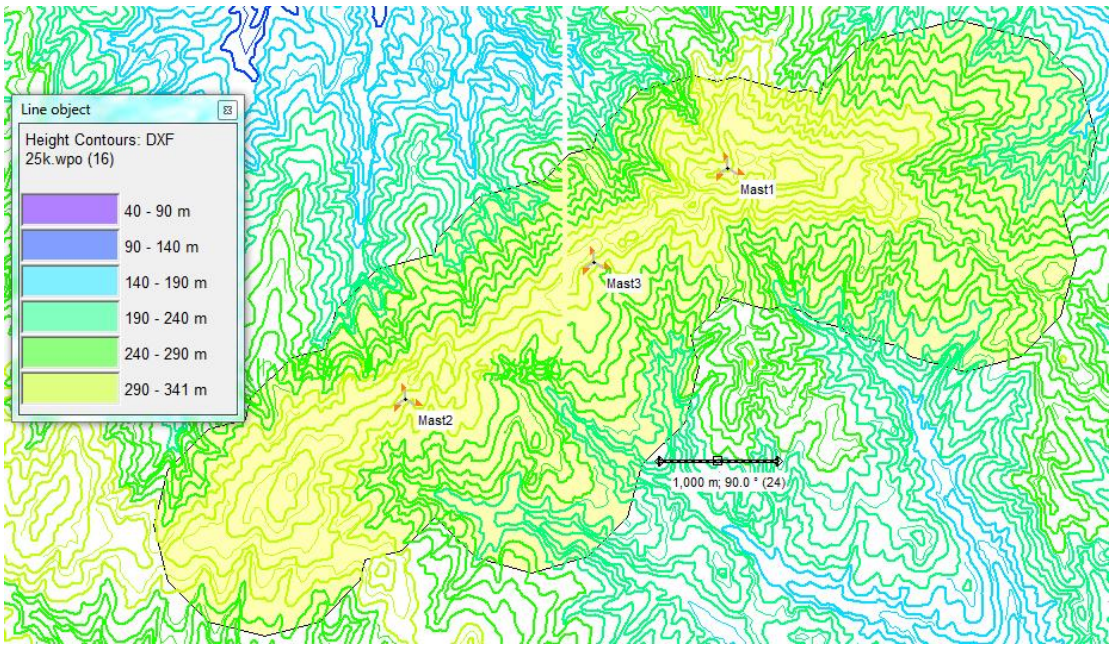


Figure 4.4. Met masts's positioning are shown with the site area on 1:25000 scale elevation map. Line is drawn in order to give an indication about the distances.

The masts are located on top of the hill which elongates in the southwest-northeast directions. Mast1 is located to the northeast part of the site at 333 m a.s.l. Mast2 is located to the southwest and at 317 m a.s.l. The mast located in the middle is Mast3 and installed at 307 m a.s.l. The heights of the used anemometers and wind vanes on the masts are shown in the table below.

Table 4.1. Height of the sensors

| | Anemometer heights (m) | Wind vane heights (m) |
|---|---|---|
| **Mast1** | 50.4 – 40.0 | 47.2 |
| **Mast2** | 80.2 – 50.0 – 20.0 | 49.8 |
| **Mast3** | 50.4 – 40.0 – 20.0 | 47.2 |

The sensors at 50.4 m for Mast 1 and Mast 3 are the top anemometers while 50.0 m sensor of Mast 2 is a side anemometer with the boom angle of 30°. Although those anemometers are the main sensor used for comparison the difference of the sensor installation and possible mast effects on the measurements are assumed to be negligible. The same approach has been followed for the other anemometers used for wind shear comparison.

In a proper site assessment study full year data is required in order to avoid the seasonal bias caused by the missing data. In this study the time series used for comparison exactly cover the same period with the available data of 9.6 months. Therefore the missing data will not be affecting the consistency of the calculations and results. For comparison the results will assumed to be representing annual wind conditions.

## 4.4. WAsP Model

WAsP (used version 11.00.0232) has been used in order to assess the wind conditions at the mast locations by other two masts individually. While setting up the model air density of 1.18 kg/m$^3$ and the standard WAsP 11 parameters [25] have been used. The use of standard parameters makes the model's atmospheric stability condition slightly stable due to the negative offset heat flux values over both land and sea. But as the measured and assessed heights above the ground are same, influence of the stability effects assumed to be negligible.

The recommendation of using elevation and roughness maps including 100xhub height or 10x10 km area around the mast and WTG locations has been fulfilled for the WAsP model.

In order to assess the wind conditions at each mast location at 50 m, three WTGs have been placed to the mast locations with the hub height of 50 m. For the energy production calculations power curve of Siemens SWT-3.0-113 has been used. Although SWT-3.0-113 does not have a 50 m hub height option this approach has been followed only for the scientific reasons. In the name of the WTG ”3.0” indicates the power output in MW and “113” indicates the rotor diameter in meters.

## 4.5. WindSim Model

In contrast to WAsP, WindSim (used version 6.0.0.24248) requires a grid file for elevation and roughness information to run the simulations. Therefore the elevation and roughness maps that have been used for WAsP calculations as well, combined and converted into a grid file. With the grid file a meshing process has been carried out. Resolution of the meshes has a big influence on the results as smaller meshes –in other words with a higher resolution- the model is able to handle the terrain effects better.

The area used for the model is 20x18 km which is sufficient for a semi-complex site. From the best practices horizontal resolution of 20-25 m mesh sizes are preferred. But for such large areas using that fine resolution requires too much computational power. Therefore an optimization between the resolution and number of cells used is needed. In order to reach the horizontal resolution of 20 m around the site area a refinement method has been applied. The aim of the refinement is to use smaller meshes around the site area as the vicinity of the objects has the most influence over the assessment results. With the refinement method 20 m horizontal resolution has been achieved for approximately 6x4 km area in the center of the model, where the objects are located. From the end of the refinement area to the edges of the model mesh sizes have gradually increased. As the importance of the resolution and terrain effects decrease with increasing distance, use of bigger meshes closer to the model boundaries is an acceptable approach to decrease the number of cells used and decrease the computational time requirement.

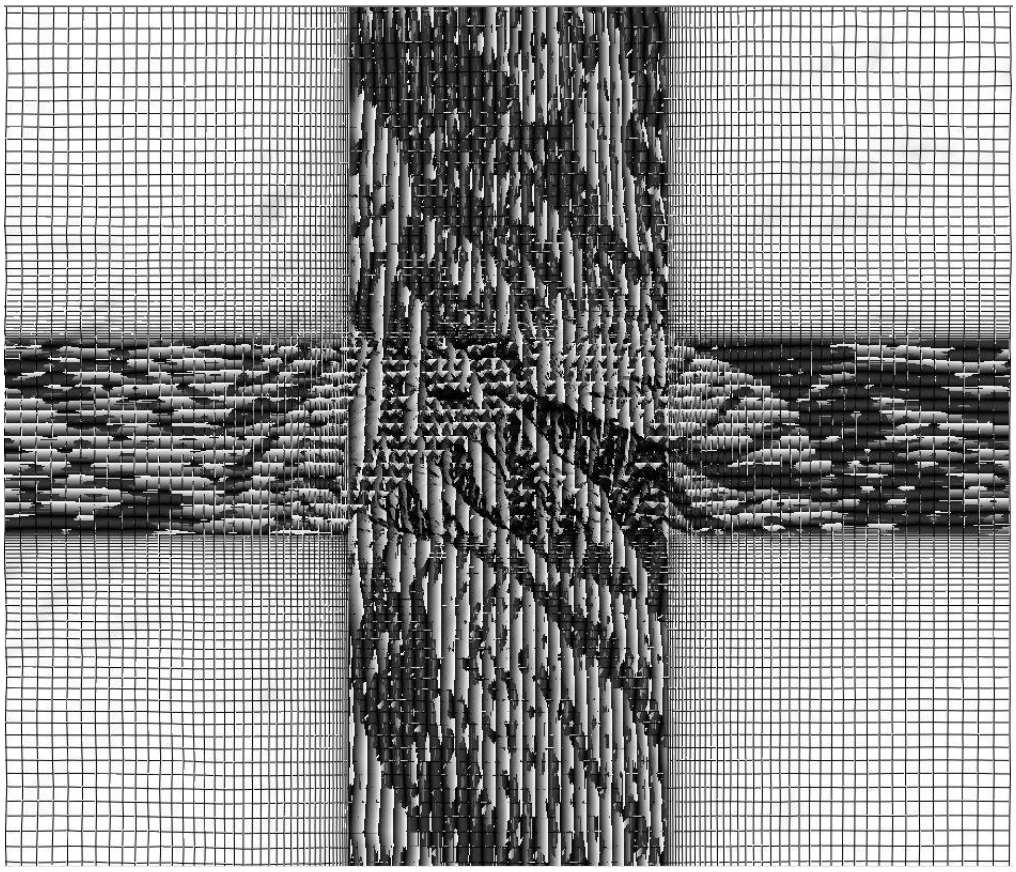

Figure 4.5. View of the horizontal resolution and refinement area. Mesh size in horizontal increases as getting closer to the boundaries.

In the below table grid spacing of 20 m indicates the grid size in the central refinement area. At the boundaries 325 m long grids have been used.

Table 4.2. Grid spacing and number of cells in x, y and z directions.

| | **x** | **y** | **z** | **total** |
|---|---|---|---|---|
| **Grid spacing, min - max (m)** | 20.0 - 325.0 | 20.0 - 325.0 | Variable | - |
| **Number of cells** | 400 | 275 | 45 | 4950000 |

Vertical resolution is also as important as the horizontal resolution but again a trade-off between number of cells and grid sizes needs to be considered. In order to catch the terrain effects better the grid sizes close to the ground should be as small as possible. But using too small grids in the vertical will require too many cells which will not be optimal in terms of computational power demands. Similar to refinement in horizontal grids, smaller cells defined in the first 100 m. After 100 m a gradual increase

applied to the cells until the upper boundary of the model which extends until 1300 m a.g.l.

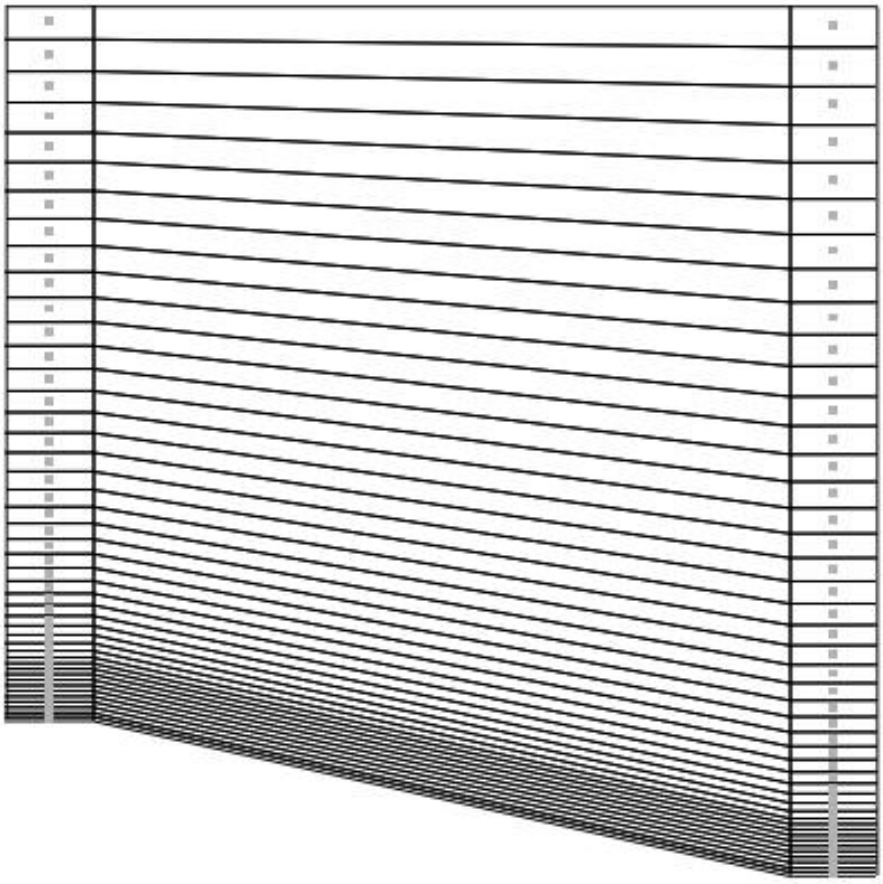

Figure 4.6. The nodes, where results from the simulations are available, are situated in the cell centers indicated by dots.

In order to match the measurement height (20, 40, 50 and 80 m approximately) vertical grids have been created with the nodes at those heights by modifying the "simple_refinement.bws" file that WindSim uses for grid refinement. As the calculations were done exactly at those heights uncertainties coming from interpolation have been avoided.

Table 4.3. Heights of the first 20 nodes a.g.l.

| **Node number** | **1** | **2** | **3** | **4** | **5** | **6** | **7** | **8** | **9** | **10** |
|---|---|---|---|---|---|---|---|---|---|---|
| **Node height (m, a.g.l.)** | 3.8 | 11.3 | 20.0 | 30.0 | 40.0 | 50.0 | 60.0 | 70.0 | 80.0 | 90.0 |
| **Node number** | **11** | **12** | **13** | **14** | **15** | **16** | **17** | **18** | **19** | **20** |
| **Node height (m, a.g.l.)** | 100.0 | 110.4 | 122.0 | 135.0 | 149.6 | 165.6 | 183.1 | 202.2 | 222.7 | 244.7 |

After creating the grids, parameters for the model setup needs to be adjusted in the "Wind Fields" module. The numerical solutions of the RANS equations are performed in this module.

Table 4.4. Main parameters adjusted in the "Wind Fields" module.

| | |
|---|---|
| **Nesting** | Disregarded |
| **Number of sectors** | 12 |
| **Height of boundary layer** | 500 |
| **Speed above boundary layer height** | 10 m/s |
| **Boundary condition at top** | Fixed pressure |
| **Potential temperature** | Disregard temperature |
| **Air Density** | 1.18 kg/m$^3$ |
| **Turbulence model** | RNG k-ε |
| **Used solver** | Segregated, coupled and GCV |

As default WindSim uses logarithmic wind profiles at the side boundaries of the model as input flow. Nesting is a method which is used for defining the boundaries from another WindSim project that covers the entire calculation area. It can also be used for taking the boundary conditions from a mesoscale meteorological model. As logarithmic profile is not always the case on sites use of nesting is useful especially when the used are is not large enough. As the area used had assumed to be large enough nesting option has been disabled for that study.

Number of sectors set as 12 as default. For more complex sites or when a specific direction results are needed to be investigated number of sectors can also be changed accordingly.

Normally atmospheric layer height and wind speeds at those heights change during the day or year. The values used for the model can be assumed as an average for the site. But with a prior knowledge about the dominant stability conditions at the site

those values can be modified accordingly. For that project atmospheric layer height and wind speed at that height have been set as default values of 500 m and 10 m/s. Those values can be considered as an average of a site with a neutral stability condition for the most of the year.

Flat and complex sites require two different treatments in WindSim. On very flat sites the pressure differences above the terrain only caused by the friction near the ground but in complex sites mainly hills and mountains set up the pressure fields. In order to avoid abrupt changes of the flow in flat terrain WindSim suggests to use no friction wall settings. To avoid unrealistic speed-ups in the complex terrain it is suggested to use fixed pressure as top boundary condition [32]. As the current site is semi-complex "Fixed pressure" has been chosen as the upper boundary condition.

Potential temperature setting can be used for the sites showing stable or unstable conditions during most of the year. In order to define the stability condition it is recommended to measure temperature at two different heights and the temperature change with height needs to be investigated. As the masts used for the study do not include two temperature measurements it is difficult to determine the stability condition at the site. Due to the lack of two temperature measurements the site assumed to show near neutral conditions for most of the year and potential temperature settings have been disabled.

Air density has been extrapolated from a nearby meteorological station to the site elevation.

RNG k-ε model has been chosen regarding to the studies of Kim and Patel [33].

Segregated solver has been used for the first run of all 12 sectors. After 3200 iterations coupled solver has been used with the results of the segregated solver. Some of the sectors diverged during the calculations and more iterations required for divergence for some other. For the diverged sectors GCV solver has been used to get the convergence. Used solvers and number of iterations run for each sector has been shown below.

Table 4.5. Used solvers and number of iterations run for each sector.

| Sectors | Used solvers & # of iterations |
|---|---|
| **0, 30, 60, 120, 150, 180, 270, 300** | Segregated: 3200, Coupled: 550 |
| **210** | Segregated: 3200, Coupled: 850 |
| **240** | Segregated:3200, Coupled: 300 |
| **90** | GCV: 900 |
| **330** | GVC: 1200 |

In WindSim convergence can be evaluated in either by setting up a convergence criteria or inspecting the spot and residual values. Convergence criteria can be set in wind fields module. When the residuals fall below the set value the calculation automatically stops. Beside convergence criteria the user can also decide by inspecting the following residuals from the convergence monitor;

- Velocity component (U1, V1 and W1)
- Turbulent kinetic energy (KE)
- Dissipation rate (EP) or the turbulent frequency (OMEG)

With the iterations the residuals are expected to decrease and reach to a negligible level which indicates that with further iterations there will be only small changes in the calculated values for the whole site at the first cell over the terrain (z=1).

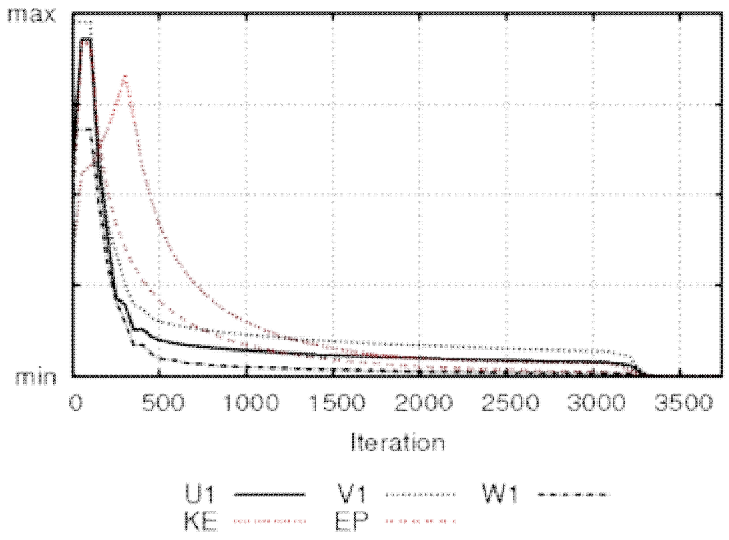


Figure 4.7. Residuals of 30° sector in the convergence monitor.

The residuals can sometimes seem to converge in overall but some parts of the site may converge slower than the other areas. In some cases even oscillation of the

flow conditions can occur. In order to catch those non-convergence issues the user can also define a spot in the area of interest (where the objects are located) and plot the residuals for that spot at the first cell over the ground.

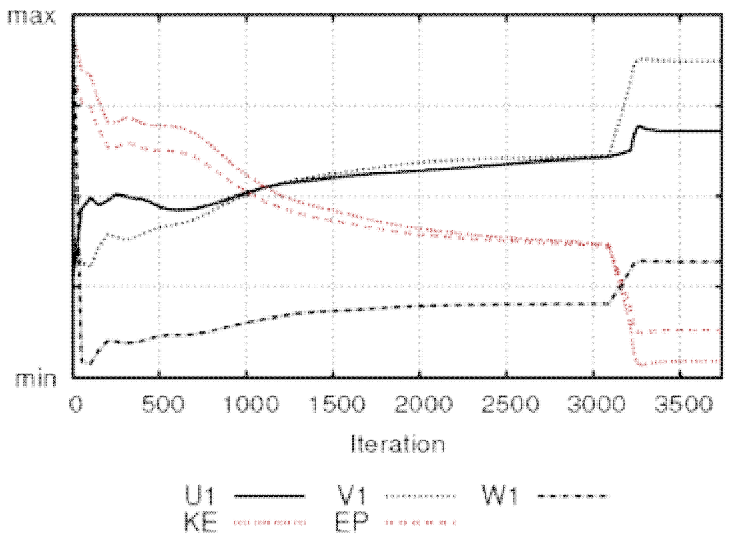


Figure 4.8. Residuals at the spot value for 30° in the convergence monitor.

Convergence of the model can also be checked from the *.vtf files that stores the field value chosen in wind fields module for each iteration and every sector for the whole area. Therefore the changes of the chosen field value can be inspected in each iteration. For this study “speed scalar XYZ” values have been inspected from those *.vtf files, calculations stopped after observing the convergence and those results have been used for further analysis.

# CHAPTER 5

# POST PROCESSING, RESULTS AND DISCUSSION

For WindSim, after running the wind fields module calculations and setting up the object locations "vertical_profile.dat" file has been created. With this file following information can be obtained at each object position;

- Height of the grids in vertical direction,
- x, y and z components of the velocity vector,
- Inflow angle,
- Derivation of 2D speed in the horizontal plane with respect to vertical direction,
- Turbulent kinetic energy,
- Turbulence intensity,
- Wind shear power exponent ($\alpha$)

Wind fields module uses the side and top boundary conditions only which are defined by the user and does not include any inputs from the measurements on site. Therefore the relationship between the objects' positions (among met masts or from mast to the WTGs) in "vertical_profile.dat" file has been used rather than the values. This relationship has been used to predict a synthetic time series at the position of interest. For this process a prediction tool has been used which was developed by Siemens Wind Power.

Basically this tool calculates the turn of the wind by using the velocity vectors between the measurement and prediction positions in "vertical_profile.dat" file. Then it calculates the change of wind speeds between two positions and finds the speed-up values. With the interpolation of wind speeds and directions in between each sector, speed-up and turn values can be found. Those speed-ups and direction values are applied to the measurement and synthetic time series are created at the prediction position.

This post processing approach can also be shown with the below flow chart;

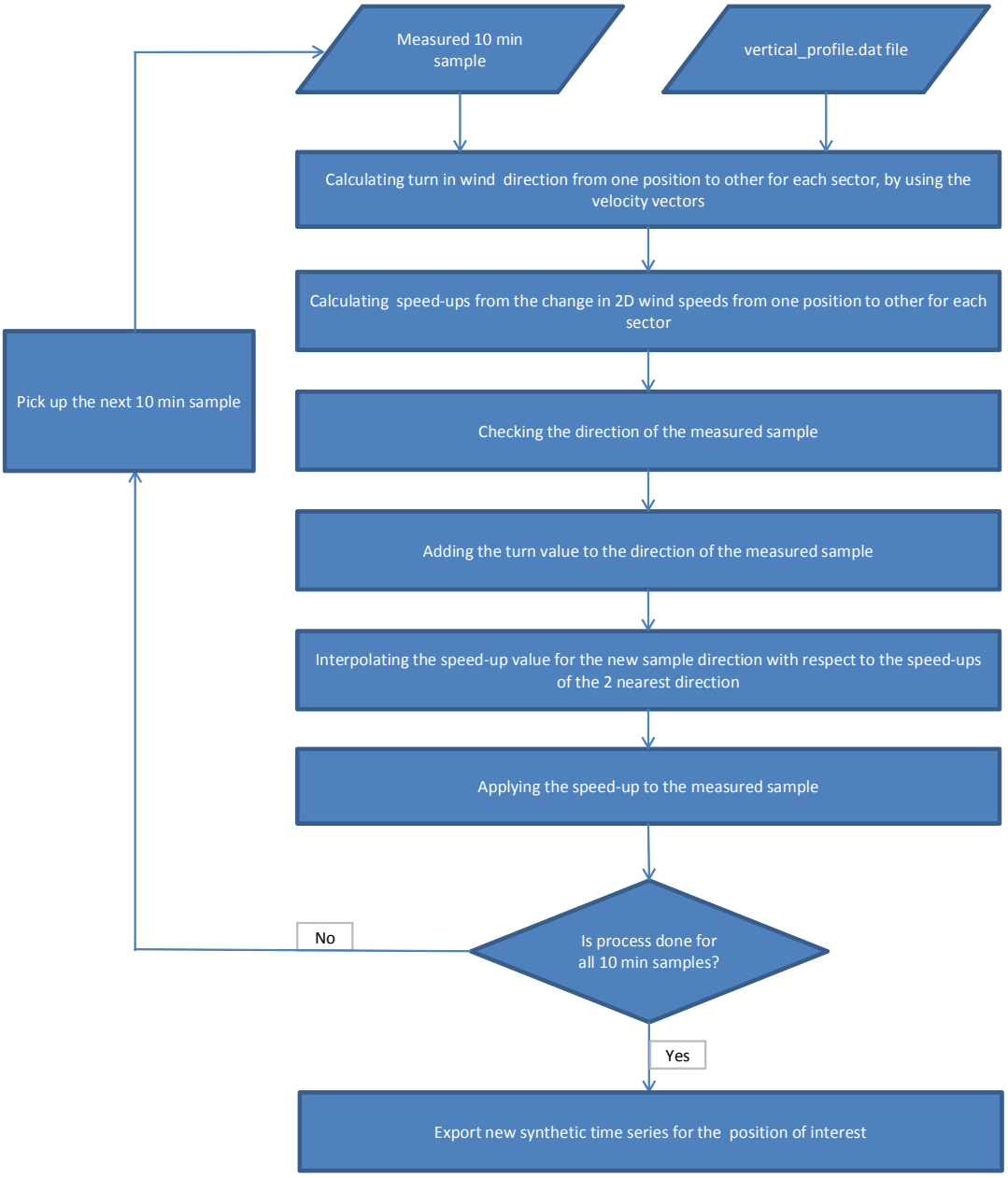


Figure 5.1. Prediction of time series by using WindSim "vertical_profile.dat" file.

After using the all three masts 6 time series have been created. The positions and names of those synthetic series are presented below;

Table 5.1. Measurement and prediction positions of the time series.

| Measured @ | Predicted @ | Shown as |
|---|---|---|
| Mast1 | Mast2 | **Mast1->2** |
| Mast1 | Mast3 | **Mast1->3** |
| Mast2 | Mast1 | **Mast2->1** |
| Mast2 | Mast3 | **Mast2->3** |
| Mast3 | Mast1 | **Mast3->1** |
| Mast3 | Mast2 | **Mast3->2** |

To evaluate the consistency of the results two error calculation methods (absolute and relative) have been used which are defined as follows;

$$e_{rel} = \sum_{i=1}^{12} \frac{\left|U_i^p - U_i^m\right|}{U_i^m} * f_i$$

$$e_{abs} = \sum_{i=1}^{12} \left|U_i^p - U_i^m\right| * f_i$$

where,

- $e_{rel}$ is relative error, in percentages,
- $e_{abs}$ is absolute error, in m/s,
- $U_i^p$ is the predicted mean wind speed of $i^{th}$ sector,
- $U_i^m$ is the measured mean wind speed of $i^{th}$ sector,
- $f_i$ is the frequency of $i^{th}$ sector,

Comparison of the each 10 minute samples has showed a relative error change between 13.64% and 21.43%. When the same approach applied for the wind speeds only between 3 and 25 m/s a significant decrease in the errors has been observed. This was an expected result as at very low wind speeds wind may not be strong enough for wind vanes and they can stand still in a random direction or rotate slowly. This might cause big wind direction deviations. As speed-up calculation is highly dependent on the direction here errors at low wind speeds are much higher.

For 3-25 m/s interval the relative error changes between 12.30% and 17.76% only. As this is the operating interval for most of the wind turbines, evaluation of the errors with this approach will give a better indication about the results.

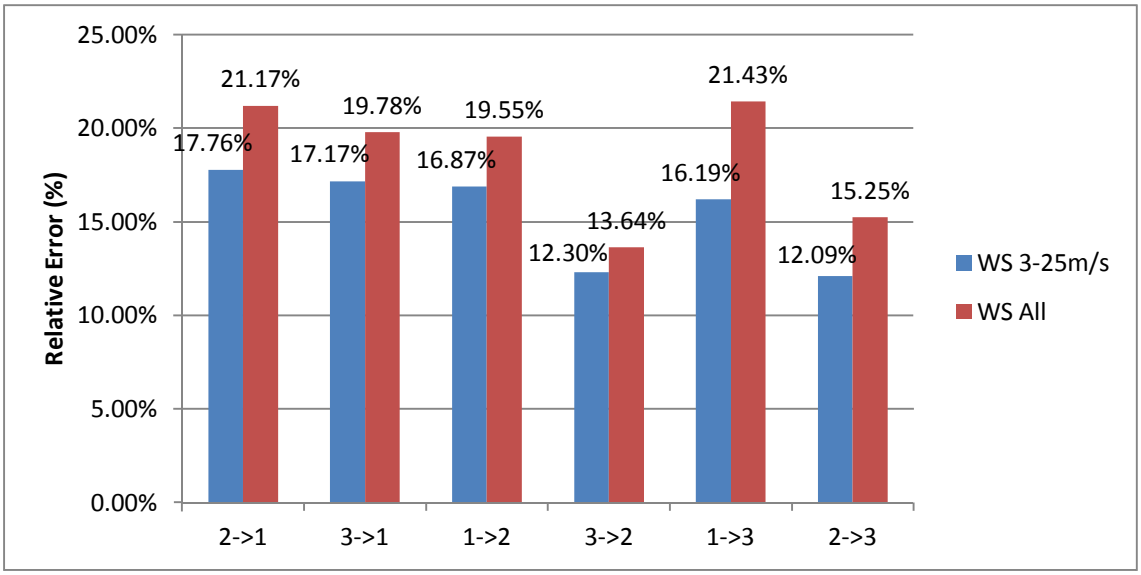


Figure 5.2. Relative errors between measured and predicted wind speeds for each 10 minute samples.

For wind direction evaluation absolute errors have been calculated. Using 3-25 m/s interval also decreases the error in direction changes.

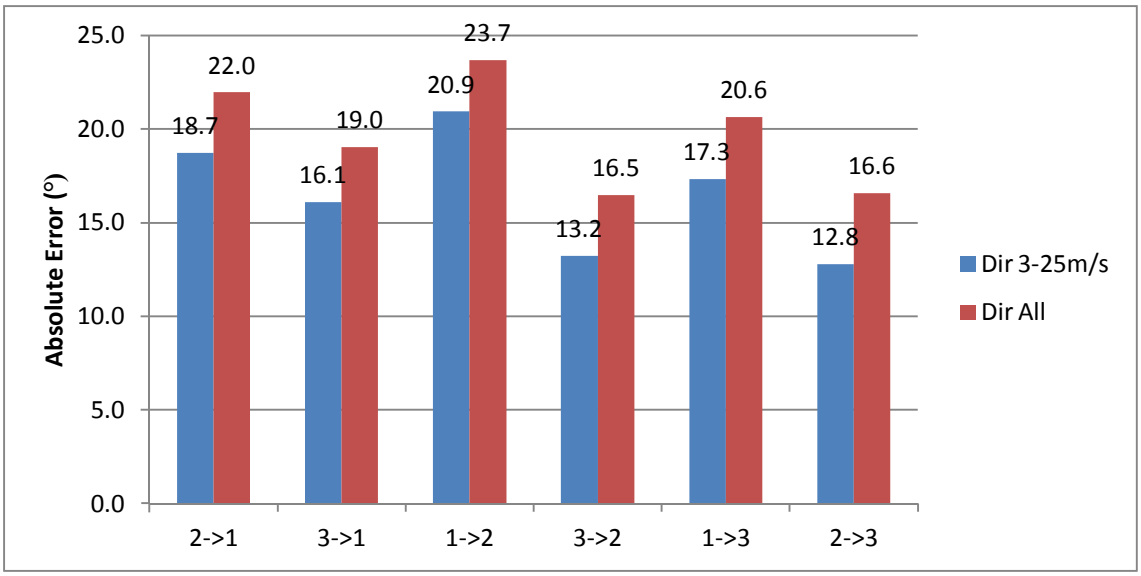


Figure 5.3. Absolute errors between measured and predicted wind directions for each 10 minute samples.

By using the measurements at one of the mast positions, WAsP methodology has also been used to predict the wind condition at the other two measurement positions

and height of 50 m. As WAsP provides sector-wise Weibull parameters for 12 sectors, frequency distributions for the measurements have been created in order to compare mean wind speeds at each sector.

The same approach has been followed for the synthetic data created with the post-processing of the WindSim results. Frequency distributions have also been created for those time series and mean wind speeds have been compared with the measurements at the same position and height.

Table 5.2. Wind speeds of the actual measurements, results of the WAsP and WindSim models at Mast2 location. Frequencies are for the actual measurements.

| MAST2 - 50 m | | | | |
|---|---|---|---|---|
| **Sector** | **Measured @Mast2** | **WAsP Mast1->Mast2** | **WindSim Mast1->Mast2** | **frequency measured** |
| **N** | 6.13 | 6.07 | 6.15 | 13.1% |
| **NNE** | 6.09 | 5.77 | 5.91 | 14.5% |
| **ENE** | 7.43 | 6.69 | 7.00 | 15.1% |
| **E** | 7.37 | 7.63 | 7.69 | 12.6% |
| **ESE** | 6.24 | 7.26 | 7.20 | 6.2% |
| **SSE** | 5.67 | 5.95 | 5.82 | 2.6% |
| **S** | 5.80 | 6.87 | 5.32 | 2.8% |
| **SSW** | 9.22 | 8.71 | 8.95 | 13.1% |
| **WSW** | 9.05 | 9.27 | 9.69 | 9.3% |
| **W** | 4.83 | 6.32 | 4.68 | 1.8% |
| **WNW** | 5.10 | 4.82 | 4.69 | 2.2% |
| **NNW** | 6.13 | 6.09 | 5.63 | 6.7% |
| **Sum** | 7.09 | 6.95 | 7.03 | 100.0% |

By using the measured and calculated sector-wise wind speeds and weighting the results with respect to the measured frequencies, below error values have been obtained at each measurement positions.

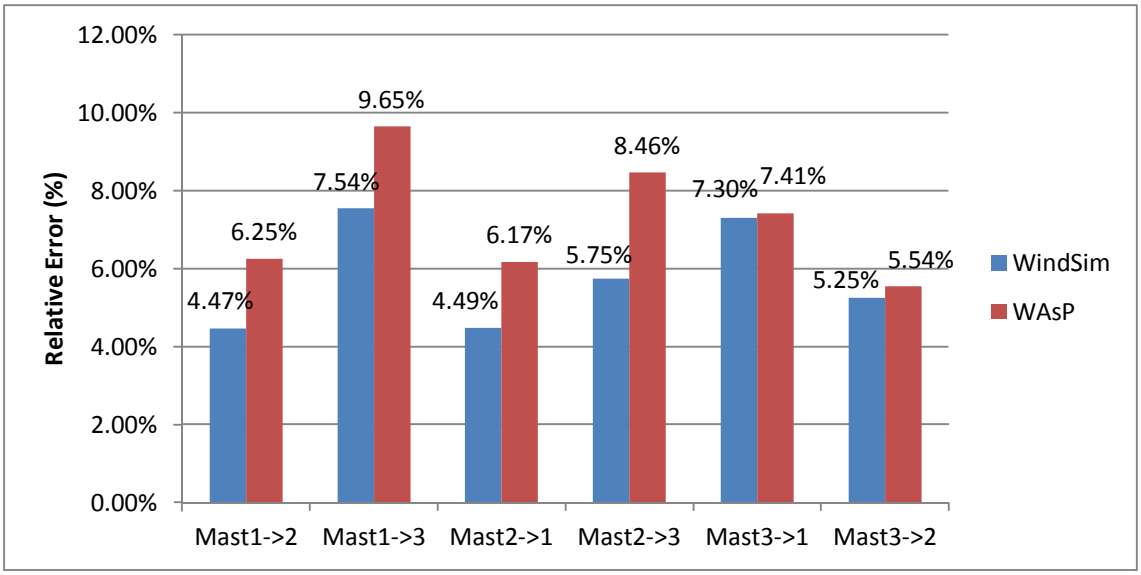


Figure 5.4. Comparison of relative error values for WindSim and WAsP results.

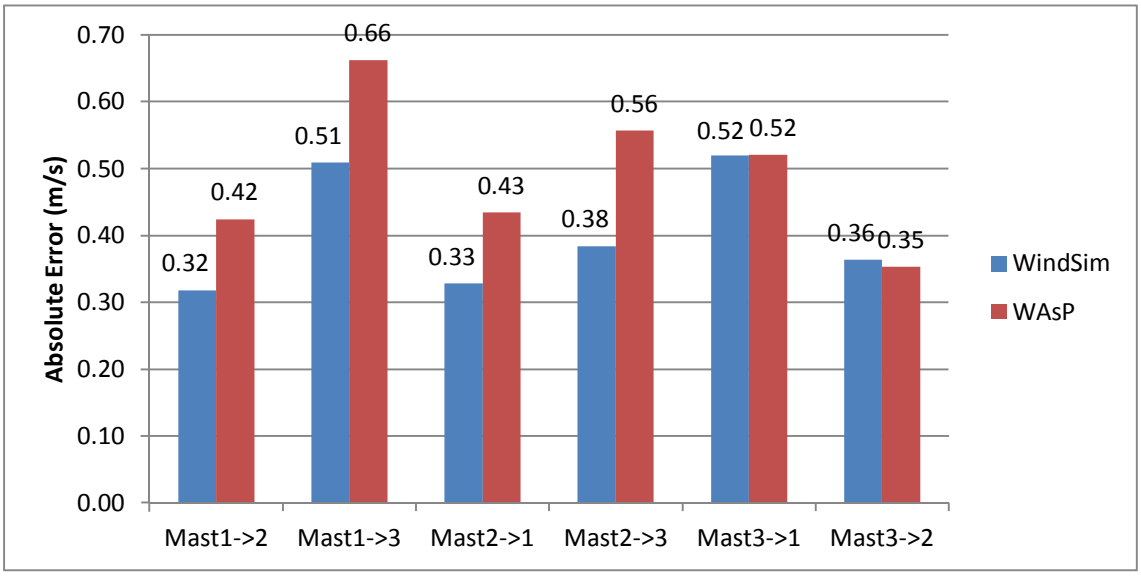


Figure 5.5. Comparison of absolute error values for WindSim and WAsP results.

At most of the sites measurements only take place at several heights which do not match the hub or tip heights. As wind conditions at those heights are necessary for energy and loads calculations it is important to model the wind shear properly with the help of available measurements. Wind shear comparison with measurements also gives remarkable pictures about consistency of the used flow model. For that reason wind shear plots of WindSim and WAsP have been compared with the measured wind speeds. As WindSim results are not scaled they have been normalized with the wind

speeds at 50 m height. For the comparison shear plots of the 2 main wind direction, N and NNE, are shown below.

Comparison of the wind shear profiles for all 12 individual sectors and overall shear values show that WAsP tends to over-predict the shear slightly while WindSim estimates lower shear coefficients. This might be the result of the stability behavior of the models. The used standard WAsP parameters make a more stable atmospheric condition in the model which creates higher wind shear over the site. As the overall shear profiles fit well with the measurements the WAsP settings assumed to be representative for the modeled area and no modification done on the heat flux parameters. In WindSim temperature equation is not activated and effects of vertical temperature distribution -which cause the buoyant forces- are not included. This causes model to run with a neutral stratification at the model's inlet and as initial conditions throughout the model. In neutral stratification case lower wind shear coefficients are expected than a stable atmosphere. This might be the reason of under-prediction of the measured shear. Hence activating the temperature equation and setting up a more stable case might help to improve model results. This study does not cover sensitivity analysis of the heat flux parameters in WAsP and temperature parameters in WindSim. Therefore a parameter sensitivity analysis can also be noted down as further improvement possibility.

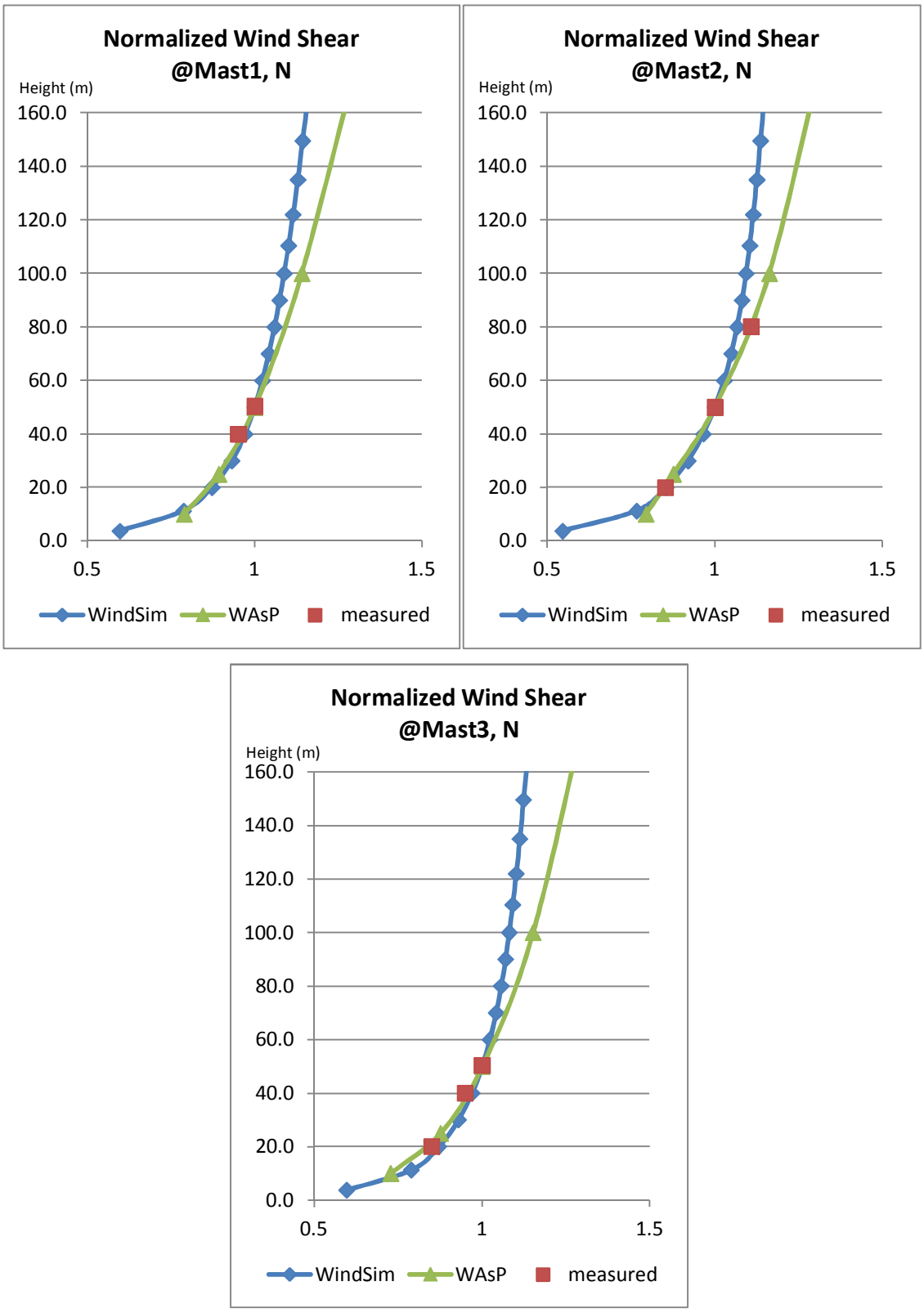


Figure 5.6. Normalized wind shear values at the mast locations in the N direction.

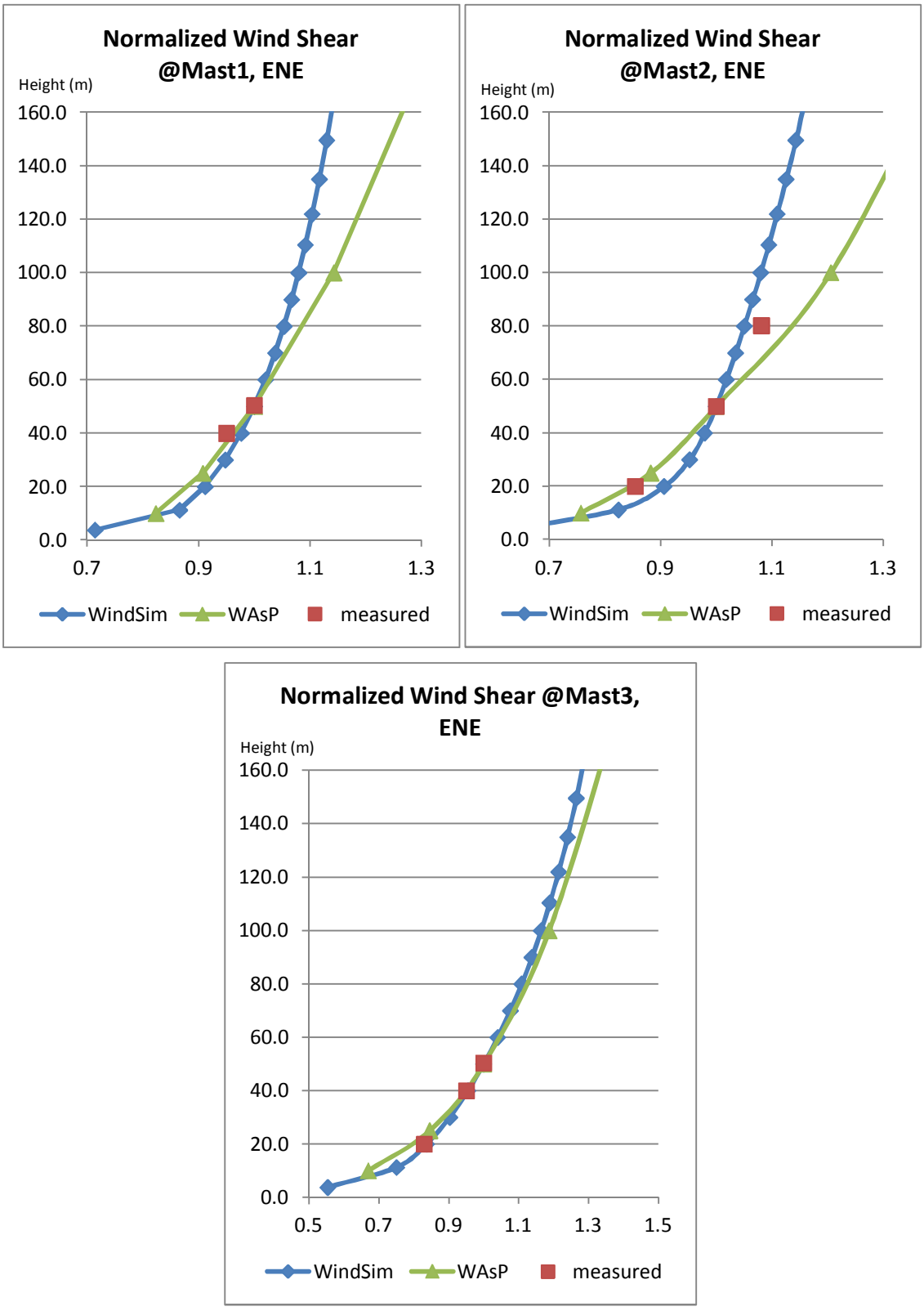


Figure 5.7. Normalized wind shear values at the mast locations in the ENE direction.

The results of WAsP and WindSim have also been compared with the measured data in terms of energy productions. For the comparison power curve of SWT-3.0-113 for the air density of 1.18 kg/m$^3$ has been used. Due to the confidentiality of the used power curve it has not been shared in details within this thesis.

SWT-3.0-113 is a Siemens direct drive wind turbine with a generator capacity of 3 MW and rotor diameter of 113 meters. The WTG has been designed for IEC IIa wind conditions. Although this WTG does not have a 50 m hub height option the power curve has only been used for scientific reasons in order to compare the productions by using the measured and predicted wind conditions at 50 m height.

The frequency distributions of the measurement data (in other words "the predictor data") and WTG power curve have been used to calculate the actual energy productions. For WindSim the frequency distribution obtained by the predicted time-series used to calculate the energy productions for each predicted positions. Finally WAsP predictions have been added to the table for the comparison.

Table 5.3. Comparison table for the energy productions.

| Measured @ | Predictor data (MWh/y) | Predictor -> Predicted | WAsP (MWh/y) | WindSim (MWh/y) |
|---|---|---|---|---|
| **Mast1** | 11436 | **2->1** | 12259 | 11755 |
| | | **3->1** | 12107 | 11455 |
| **Mast2** | 10739 | **1->2** | 10146 | 10339 |
| | | **3->2** | 10802 | 10618 |
| **Mast3** | 10323 | **1->3** | 9798 | 9991 |
| | | **2->3** | 10370 | 10351 |

For the comparison of the annual energy productions relative errors have been calculated but the absolute values have not taken in order to show if the prediction is higher or lower than the measurement results. Therefore the used relative error equations takes the below form.

$$e = \frac{(AEP^p - AEP^m)}{AEP^m}$$

where,

- e is relative error, in percentages,
- $AEP^p$ is the annual energy production at the predicted position,
- $AEP^m$ is the annual energy production at the measured position.

The relative error values calculated with this approach is also shown below.

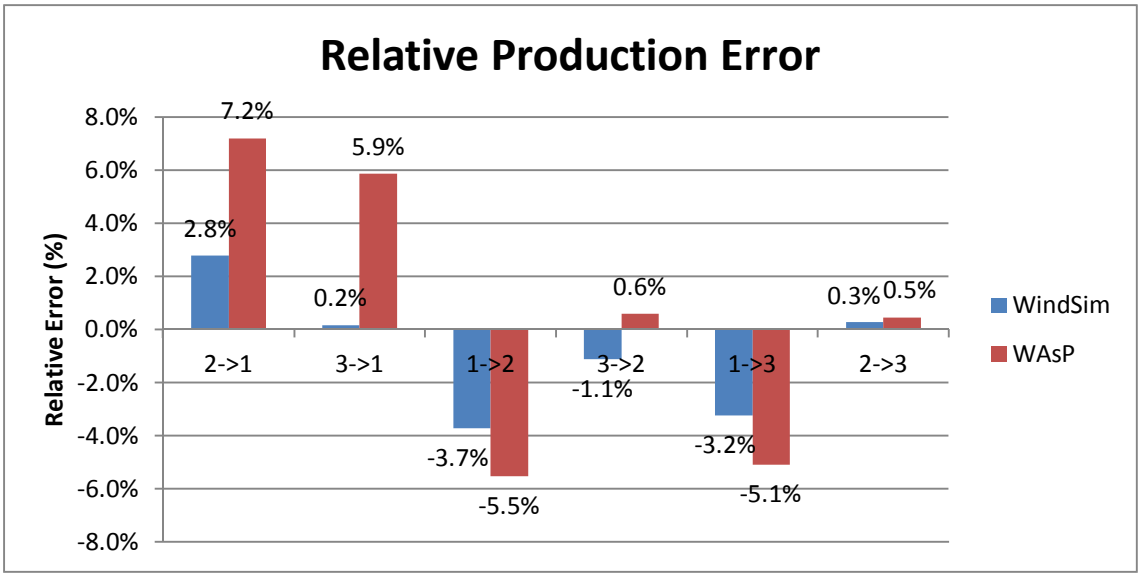


Figure 5.8. Relative production errors of the results.

The results show that minimum prediction errors occur between Mast2 and Mast3. But prediction errors with Mast1 are higher in overall for both models. Mast2 and Mast3 tend to over-estimate the energy production at Mast1 position. In general WindSim results seem to show lower error values than WAsP. One of the reasons for that is the effects of roughness are higher in the WAsP model in which the roughness lengths are slightly overestimated especially for the forested areas. Although the suggested roughness length of 0.6 m for the forested areas in [31] has been modified as 0.4 m for the vicinity of the masts the speed-down effects on Mast2 and Mast3 in the main wind directions of north and north-east still seem to be high. Those roughness effects are lower at Mast1 as this location have lower roughness elements and less forested areas in the same directions. Therefore decreasing the roughness lengths for the forested areas all over the site might be another improvement for this study. For any further studies this general classification of roughness length by land cover data should be used carefully as an outcome of those results.

The average of the absolute energy errors for WAsP and WindSim are 4.2% and 1.8% respectively. The WindSim model is performing better for all of the energy predictions and the energy predictions can be considered as in an acceptable error level. But this study is the first and only test case for where this WindSim post-processing method has been applied. In addition to that there are only one WAsP and WindSim models have been used within this study. Therefore the suggested model modifications given throughout the thesis should be applied and other test cases sites with higher site complexity should be assessed with the same methodologies before concluding that any of the flow models are better than the other one.

# CHAPTER 6

# CONCLUSION

Comparison for wind speed results of the WindSim model with the measurements on 10 minute basis gives relative average values between 12.09% and 17.76%. Those are quite high values when compared to the results of relative errors for annually averaged wind speeds. WindSim model calculations are done for certain flow assumptions (such as the defined boundary or stability conditions) which each 10 minute condition cannot fit with. Therefore dominant flow conditions for the site should be chosen while setting up the model and annual averaged wind speeds and directions should be used for the assessment procedure.

Although it is not shown in detail in this study, the relative and absolute error values for wind direction (and in predicted wind speeds as they are also dependent on the direction) have tendency to decrease as the wind speeds increase around 11-12 m/s levels. For lower wind speeds (up to 3-5 m/s) wind-independent turn of wind vanes has high influence on the high error values. For higher wind speeds (above 5 m/s) the mismatch of the measured and predicted directions is mainly the result of mismatch of model assumptions and flow conditions and gives a better indication about the capability of the model to simulate the flow.

Importance of the roughness increases as the orographic complexity decreases for the WAsP model. Roughness input plays an important role on the calculation results for such semi-complex or simple sites. This can be observed in the relative prediction between Mast1 and Mast2&3 and as explained in Chapter 5.

Relative and absolute errors in sector-wise model results have been weighted with the frequency of the measurements. This is a convenient approach in order to understand how good the predictions are after averaging into sectors. But energy productions are not only related with the frequency but also to wind speeds. Therefore a full relationship between the wind speed and energy production errors could not be obtained.

In the comparison of the normalized wind shear values the difference is expected to be the result of the different stability assumptions of default settings of WAsP and

WindSim. In order the modify the models with respect to the sites dominant stability conditions the proper approach would be to make two temperature measurements at different heights and observe the temperature difference during the year. As those measurements were not available best possible approach is to modify heat flux settings for WAsP and activate the energy equation for WindSim with the light of achieved shear results in that calculation. An improvement on the shear fits might be possible by decreasing the offset heat flux over land for WAsP or setting up a positive Monin-Obukhov Length for WindSim.

Wind Speed and energy prediction errors for WindSim are lower than WAsP model results in general for the assessed models and with used approaches. Although the results point that non-linear model works better here the expected error differences were lower for such semi-complex sites as the known weaknesses of linear models are observed in the complex sites and caused by the simplified linearization of the advection terms and the other weaker nonlinearities in the turbulence closure equation. Therefore further modification of the models and use of different test cases as suggested throughout the thesis will be important for a better understanding the relation of the used model and energy prediction errors. Same suggestions apply for further validation of the used post-processing tool for WindSim.

# REFERENCES


[1] R. Pereira, R. Guedes, C.S. Santos, *Comparing WAsP and CFD wind resource estimates for the regular user,* EWEC, Warsaw, 2010.

[2] J.M.L.M Palma, F.A. Castro, L.F. Ribeiro, A.H. Rodrigues, A.P. Pinto, *Linear and nonlinear models inwind resource assessment and wind turbine micro-siting in complex terrain*, Journal of Wind Engineering and Industrial Aerodynamics 96, pp. 2308– 2326, 2008.

[3] K.W. Ayotte, *Computational modelling for wind energy assessment*, Journal of Wind Engineering and Industrial Aerodynamics 96, 2008.

[4] K.W. Ayotte, R.J. Davy, P.A. Coppin, *A simple temporal and spatial analysis of flow in complex terrain in the context of wind energy modelling*, 2001.

[5] G. D. Ahrens, *Meteorology today: An introduction to weather, climate, and the enviroment*, Brooks/Cole, Cengage Learning, 2009.

[6] http://www.physicalgeography.net/, 2013.

[7] http://www.srh.noaa.gov/, 2013.

[8] http://www.meteo.psu.edu/, 2013.

[9] http://en.wikipedia.org/wiki/Wind, 2013.

[10] J. C. Kaimal, J. J. Finnigan, *Atmospheric boundary layer flows: their structure and measurement*, Oxford University Press, New York, NY, 1994.

[11] http://www.wind-energy-the-facts.org/, 2013.

[12] http://en.wikipedia.org/wiki/Ekman_layer, 2013.

[13] R.B. Stull, *An introduction to boundary layer meteorology*, Kluwer Academic Publishers, 1988.

[14] C. Meissner, A. R. Gravdahl, B. Steensen, *Including thermal effects in CFD simulations*, Brussels, EWEC, 2009.

[15] M. Mohan, T. A. Siddiqui, *Analysis of Various Schemes for the Estimation of Atmospheric Stability Classification*, Atmospheric Enviroment Vol. 32, No. 21, pp. 3775-3781, 1998.

[16] R. Gasch,.J. Twele, *Wind power plants: Fundamentals, design, construction and operation,* 2nd Edition, Springer, 2012.

[17] T. Troen, E. Peterson, *European wind atlas*, Risø National Laboratory, Roskilde, Denmark, 1989.

[18] T. Burton, D.Sharpe, N. Jenkins, E. Bossanyi, *Wind energy handbook* John Wiley & Sons, 2001.

[19] IEC 61400-1, *Wind turbines-Part 1: Design requirements*, 2005.

[20] MEASNET, *Evaluation of site-specific wind conditions*, Version 1, 2009.

[21] MEASNET, *Anemometer calibration procedure*, Version 2, 2009.

[22] IEC61400-12-1, *Power Performance Measurements of Electricity Producing Wind Turbines*, 2005.

[23] S. Lang, E. McKeogh, *LIDAR and SODAR Measurements of Wind Speed and Direction in Upland Terrain for Wind Energy Purposes,* Remote Sensing – Open Access Journal ISSN 2072-4292, 2011.

[24] P.A.Taylor, H.W.Teunissen, *The Askervein Hill Project: Vertical profiles of wind and turbulence*, Boundary Layer Meteorology, Volume 43, issue 1-2, pp. 143-169, 1987.

[25] *WAsP 11 Help Facility and On-line Documentation*, Department of Wind Energy, Technical University of Denmark, 2013.

[26] T. Wallbank, *WindSim validation study – CFD validation in complex terrain*, WindSim, 2008.

[27] E. Berge et al, *Wind in complex terrain – A comparison of WAsP and two CFD-models*, EWEC, Athens, 2006.

[28] A. Bakker, *Turbulence modeling notes*, ed: http://www.bakker.org/, 2013.

[29] G. Crasto, *Numerical simulations of the atmospheric boundary layer*, Universita degli Studi di Cagliari, 2007.

[30] *WAsP Best Practices and Checklist*, Department of Wind Energy, Technical University of Denmark, 2009

[31] J. Silva, C. Ribeiro, R.Guedes, Roughness length classification of corine land cover classes, EWEC, Milan, 2007.

[32] WindSim User Area, http://user.windsim.com/, 2013

[33] H. G. Kim, V. C. Patel, *Test of turbulence models for wind flow over terrain with seperation and recirculation*, Iowa Institute of Hydraulic Research, The University of Iowa, 1999.